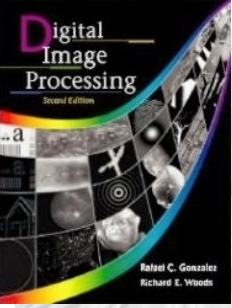


Chapter 7

Wavelets and Multiresolution Processing

- Wavelet transform vs Fourier transform
- Basis functions are small waves called *wavelet* with *different frequency* and *limited duration*
- Multiresolution theory: representation and analysis of signals/images at more than one resolutions.
 - Subband coding
 - Quadrature mirror filtering
 - Pyramid image processing

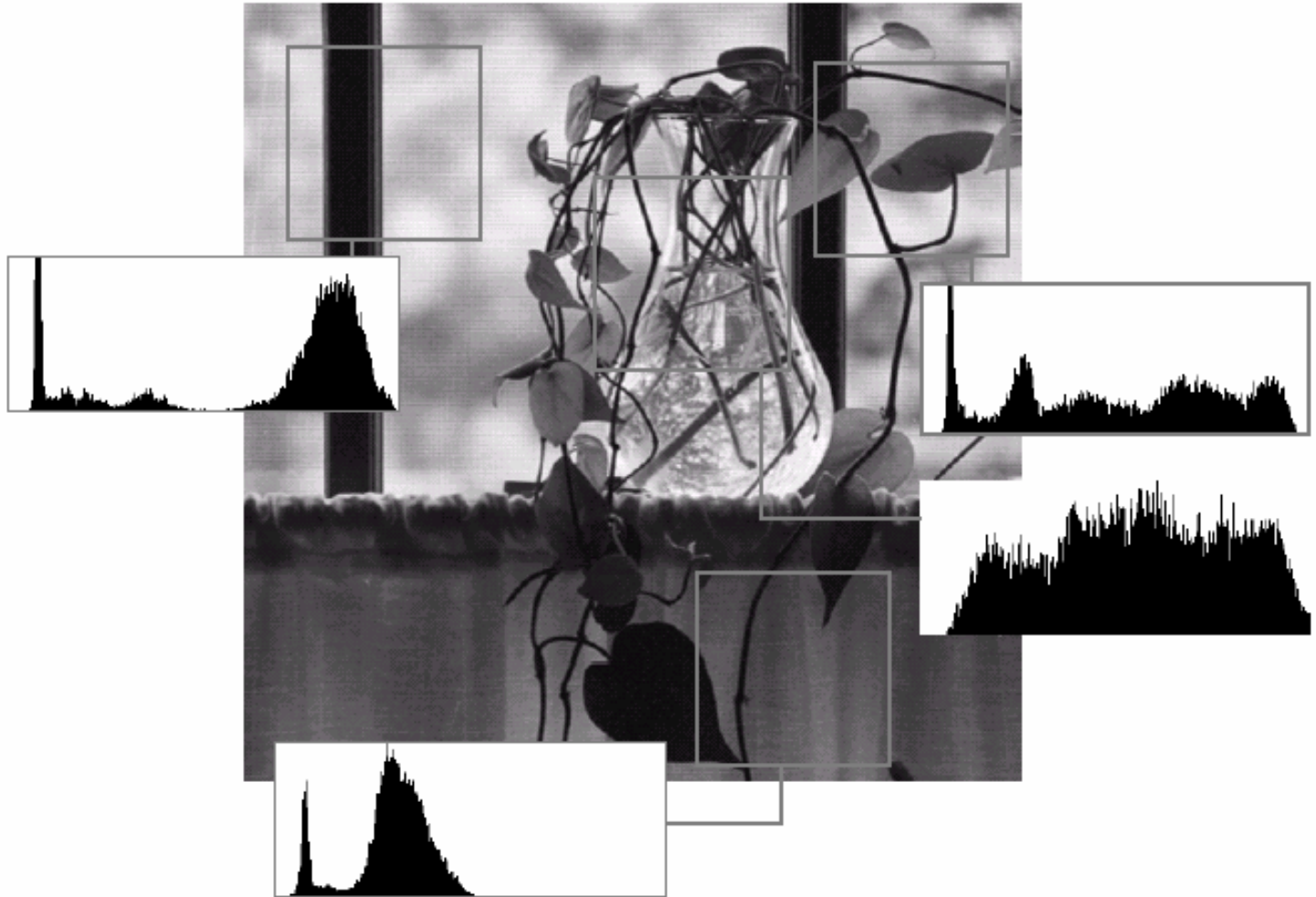


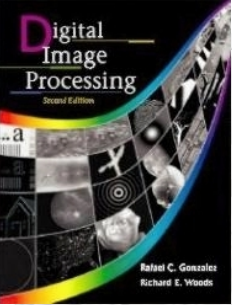
7.1 Background

- Small objects or low contrast images are examined at high resolutions; whereas large object and high contrast images are examined in low resolution.
- Images are 2-D array of intensity with locally varying statistics

7.1 Background

FIGURE 7.1 A natural image and its local histogram variations.

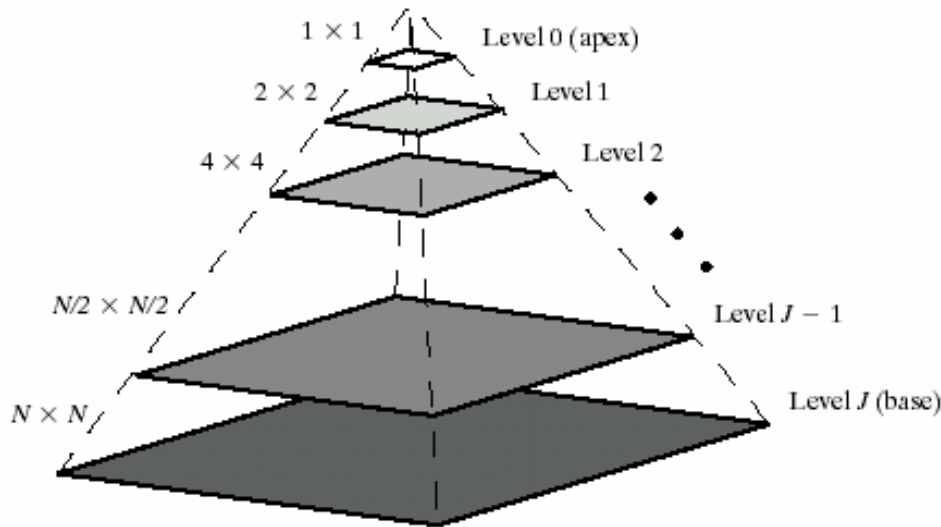




7.1 Background

- **Image Pyramids**
- Base level J with size $2^J \times 2^J$ or $N \times N$ where $J = \log_2 N$
- Intermediate level j with size $2^j \times 2^j$ with $0 \leq j \leq J$
- Most pyramids are truncated to $P+1$ levels where $j = J-P, \dots, J-1, J$
- The total number of pixel elements in a $P+1$ level pyramid is
$$N^2 \left(1 + \frac{1}{4^1} + \frac{1}{4^1} + \dots + \frac{1}{4^P} \right) \leq \frac{4}{3} N^2$$

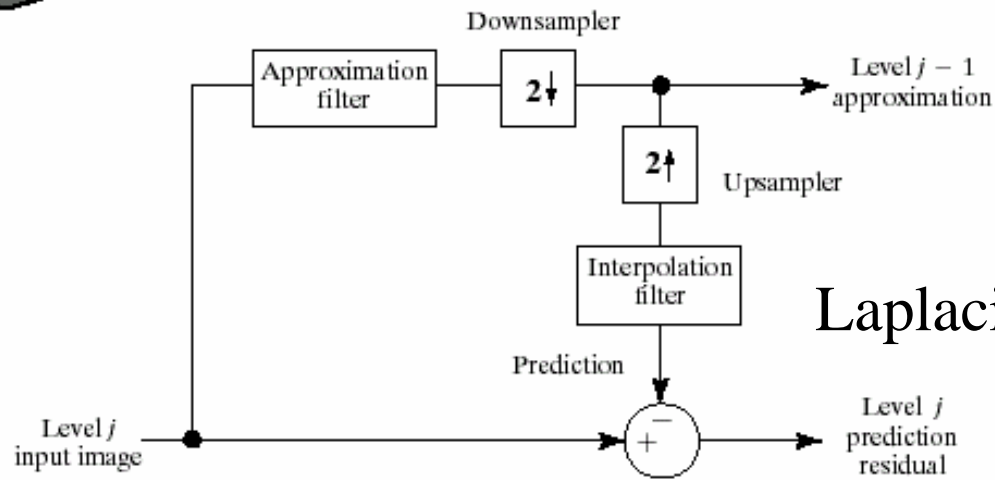
7.1 Background



a
b

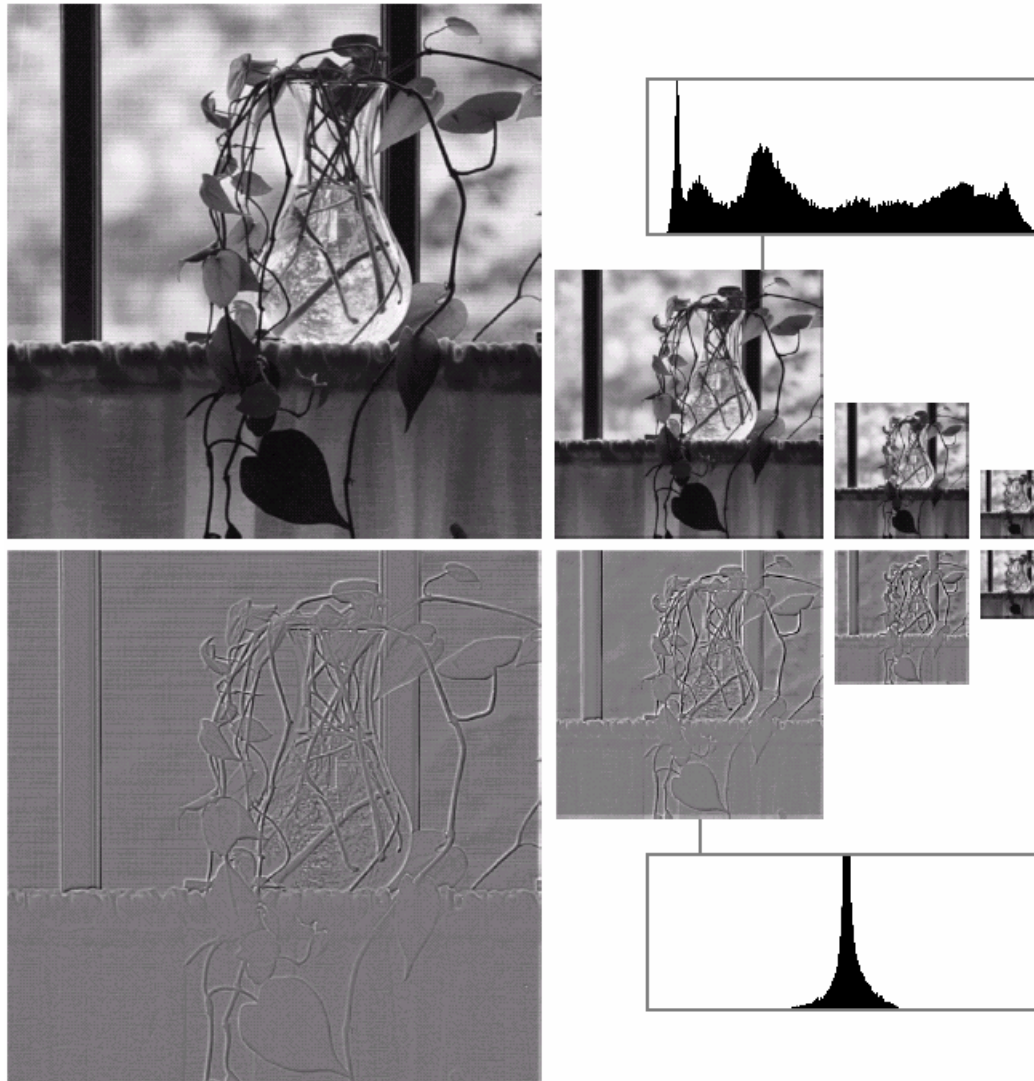
FIGURE 7.2 (a) A pyramidal image structure and (b) system block diagram for creating it.

Gaussian pyramid

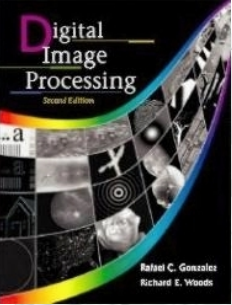


Laplacian Pyramid

7.1 Background

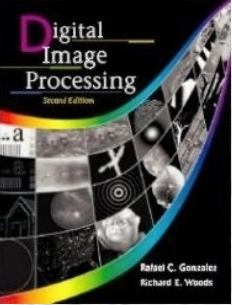


a
b
FIGURE 7.3 Two image pyramids and their statistics: (a) a Gaussian (approximation) pyramid and (b) a Laplacian (prediction residual) pyramid.



7.1 Background-Subband Coding

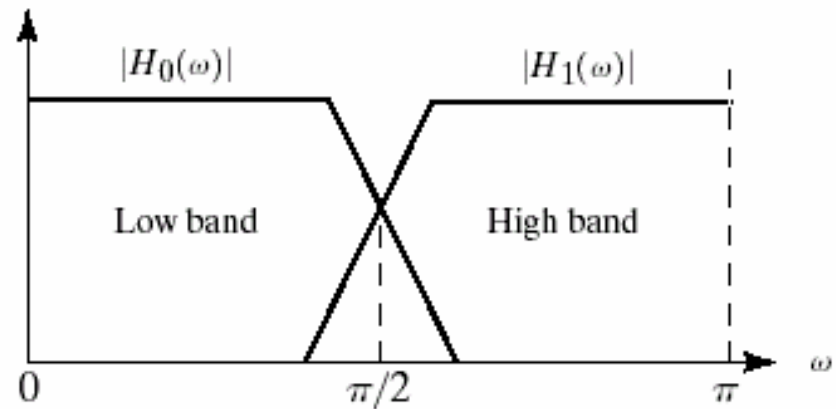
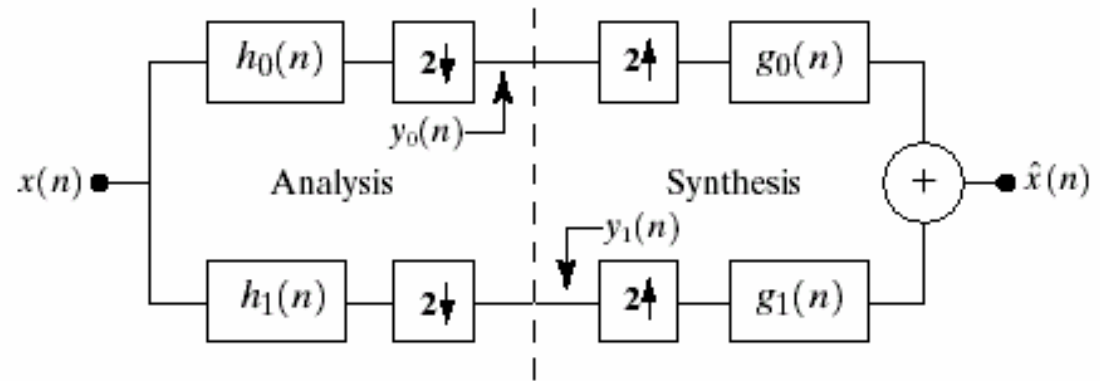
- In subband coding: an image is decomposed into a set of bandlimited components, called subbands.
- The subbands can be downsampled without loss of information.
- Reconstruction of the original image is accomplished by upsampling, filtering, and summing the individual subbands

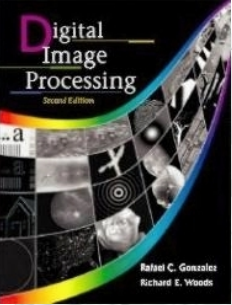


7.1 Background-Subband Coding

a
b

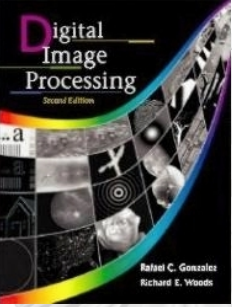
FIGURE 7.4 (a) A two-band filter bank for one-dimensional subband coding and decoding, and (b) its spectrum splitting properties.





7.1 Background-Subband Coding

- The input is 1-D band-limited discrete time signals $x(n)$, $n=0,1,2,\dots$
- *The output $\hat{x}(n)$ is formed through the decomposition of $x(n)$ into $y_0(n)$ and $y_1(n)$ via analysis filter $h_0(n)$ and $h_1(n)$, and subsequent recombination via synthesis filters $g_0(n)$ and $g_1(n)$.*
- *The Z-transform of $x(n)$ is $X(z) = \sum_{-\infty}^{\infty} x(n)z^{-n}$*
- $x_{down}(n)=x(2n) \quad X_{down}(z)=1/2[X(z^{1/2})+X(-z^{1/2})]$
- $x_{up}(n)=x(n/2)$ for $n=0,2,4,.. \quad X_{up}(z)=X(z^2)$



7.1 Background-Subband Coding

- $\hat{x}(n)$ is obtained from the downsampled and upsampled $x(n)$, therefore

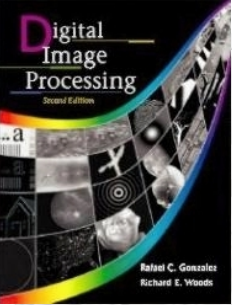
- $$\hat{X}(z) = \frac{1}{2} [X(z) + X(-z)]$$

- $X(-z)$ is the modulated version of $x(n)$

- $Z^{-1} [X(-z)] = (-1)^n x(n)$

- *The system output is*

$$\begin{aligned} \hat{X}(z) = & \frac{1}{2} G_0(z) [H_0(z) X(z) + H_0(-z) X(-z)] \\ & + \frac{1}{2} G_1(z) [H_1(z) X(z) + H_1(-z) X(-z)] \end{aligned}$$

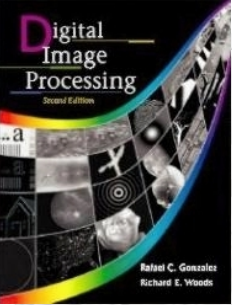


7.1 Background-Subband Coding

- Rearrange
$$\hat{X}(z) = \frac{1}{2} [H_0(z)G_0(z) + H_1(z)G_1(z)]X(z) + \frac{1}{2} [H_0(-z)G_0(z) + H_1(-z)G_1(z)]X(-z)$$
- The second component contain the $-z$ dependence, represents the aliasing that is introduced by downsampling-upsampling process.
- For error-free reconstruction of the input, $x(n) = \hat{x}(n)$
- The second component is zero.

$$H_0(-z)G_0(z) + H_1(-z)G_1(z) = 0$$

$$H_0(z)G_0(z) + H_1(z)G_1(z) = 2$$



7.1 Background-Subband Coding

- Reduce to matrix expression

$$\begin{bmatrix} G_0(z) & G_1(z) \end{bmatrix} \mathbf{H}_m(z) = \begin{bmatrix} 2 & 0 \end{bmatrix}$$

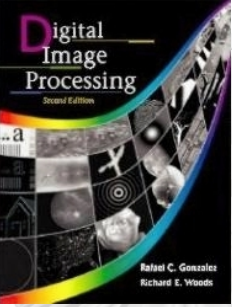
- Where

$$\mathbf{H}_m(z) = \begin{bmatrix} H_0(z) & H_0(-z) \\ H_1(z) & H_1(-z) \end{bmatrix}$$

- Assume that $\mathbf{H}_m(z)$ is nonsingular then

$$\begin{bmatrix} G_0(z) \\ G_1(z) \end{bmatrix} = \frac{2}{\det(\mathbf{H}_m(z))} \begin{bmatrix} H_1(-z) \\ -H_0(-z) \end{bmatrix} \quad (7-12)$$

- The analysis and synthesis filtered are cross-modulated.



7.1 Background-Subband Coding

- For FIR filters, the determinate of the modulation matrix is a pure delay, i.e.,

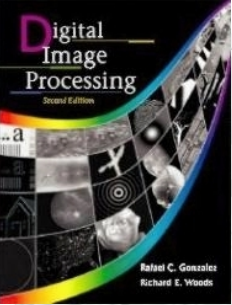
$$\det(\mathbf{H}_m(z)) = \alpha z^{-(2k+1)}$$

- Ignoring the delay and let $\alpha=2$, by taking inverse Z transform we have

$$g_0(n) = (-1)^n h_1(n) \quad \text{and} \quad g_1(n) = (-1)^{n+1} h_0(n)$$

- If $\alpha=-2$ then

$$g_0(n) = (-1)^{n+1} h_1(n) \quad \text{and} \quad g_1(n) = (-1)^n h_0(n) :$$



7.1 Background-Subband Coding

- *The biorthogonality of the analysis and synthesis filters, let $P(z)$ be the product of the lowpass analysis and synthesis filter from (7.12)*

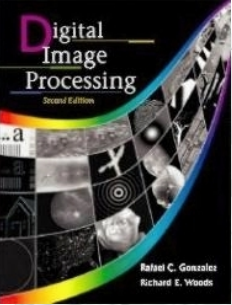
$$P(z) = G_0(z)H_0(z) = 2H_0(z)H_1(-z)/\det(\mathbf{H}_m(z))$$

also $\det(\mathbf{H}_m(z)) = -\det(\mathbf{H}_m(-z))$

and $G_1(z)H_1(z) = -2H_0(-z)H_1(z)/\det(\mathbf{H}_m(z)) = P(-z)$

Thus $G_1(z)H_1(z) = P(-z) = G_0(-z)H_0(-z)$

and $G_0(-z)H_0(-z) + G_0(-z)H_0(-z) = 2$



7.1 Background-Subband Coding

- Inverse z-transform

$$\sum g_0(k)h_0(n-k) + (-1)^n \sum g_0(k)h_0(n-k) = 2\delta(n)$$

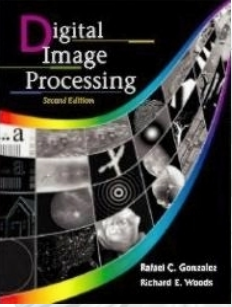
- Odd index terms cancel, it is simplified as

$$\sum g_0(k)h_0(2n-k) = \langle g_0(k), h_0(2n-k) \rangle = \delta(n)$$

- Express G_0 and H_0 as function of G_1 and H_1

$$\langle g_1(k), h_1(2n-k) \rangle = \delta(n), \quad \langle g_0(k), h_1(2n-k) \rangle = 0$$

$$\langle g_1(k), h_0(2n-k) \rangle = 0$$



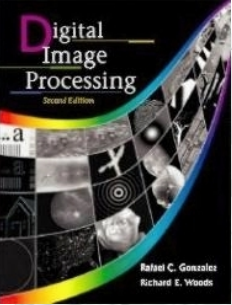
7.1 Background-Subband Coding

- More general expression:

$$\langle g_j(k), h_i(2n-k) \rangle = \delta(i-j)\delta(n) \quad i, j = \{0, 1\} \quad (7.21)$$

- Filter banks satisfying this condition are **bi-orthogonal**
- Quadrature mirror filter(QMF) (Table 7.1)
- Conjugate quadrature filter (CQF) (Table 7.1)
- Orthonormal filter (Table 7.1) for *fast wavelet transform*, it requires that (7.22)

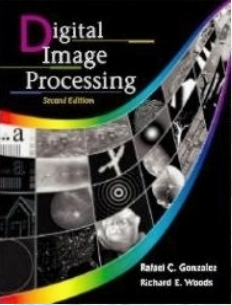
$$\langle g_i(n), g_i(n+2m) \rangle = \delta(i-j)\delta(m) \quad i, j = \{0, 1\}$$



7.1 Background-Subband Coding

Filter	QMF	CQF	Orthonormal
$H_0(z)$	$H_0^2(z) - H_0^2(-z) = 2$	$H_0(z)H_0(z^{-1}) + H_0^2(-z)H_0(-z^{-1}) = 2$	$G_0(z^{-1})$
$H_1(z)$	$H_0(-z)$	$z^{-1}H_0(-z^{-1})$	$G_1(z^{-1})$
$G_0(z)$	$H_0(z)$	$H_0(z^{-1})$	$G_0(z)G_0(z^{-1}) + G_0(-z)G_0(-z^{-1}) = 2$
$G_1(z)$	$-H_0(-z)$	$zH_0(-z)$	$-z^{-2K+1}G_0(-z^{-1})$

TABLE 7.1
Perfect reconstruction filter families.



7.1 Background-Subband Coding

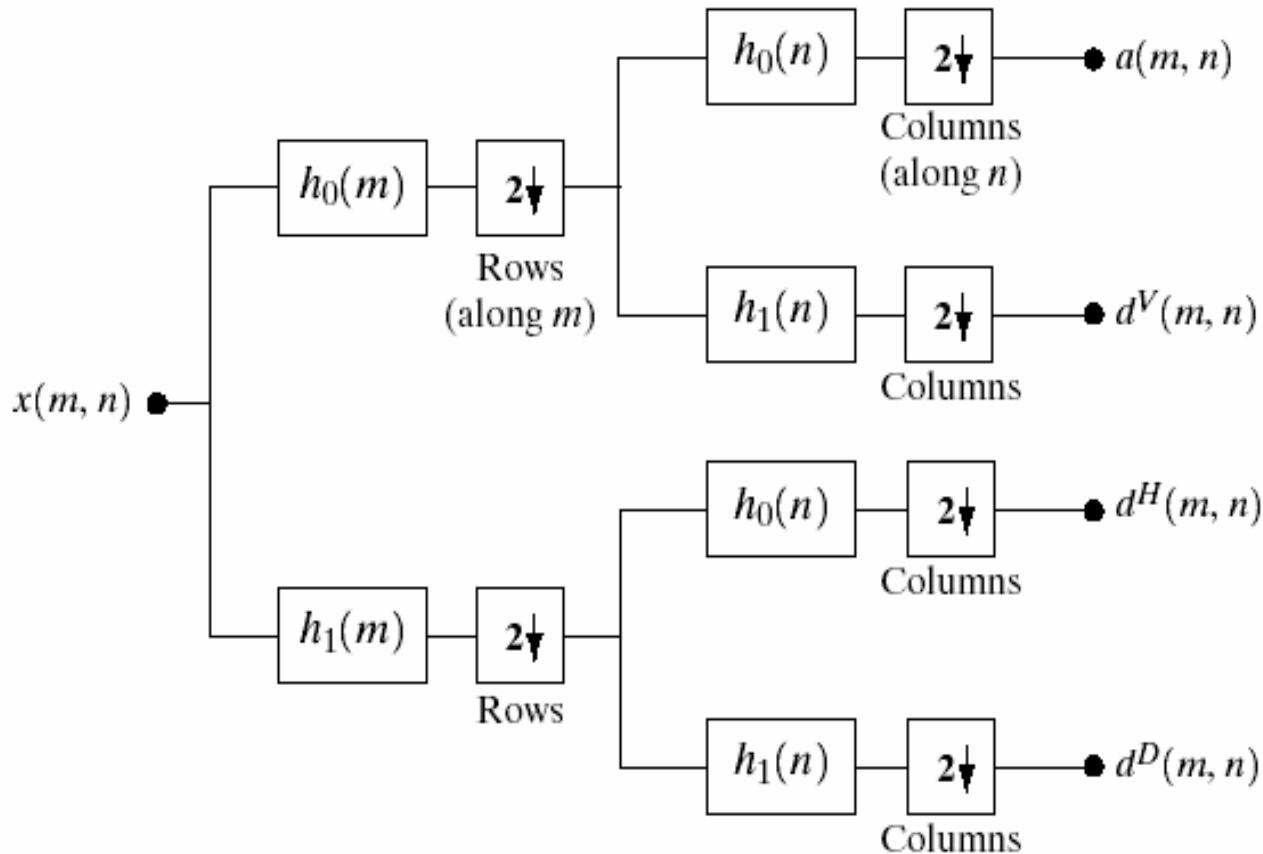
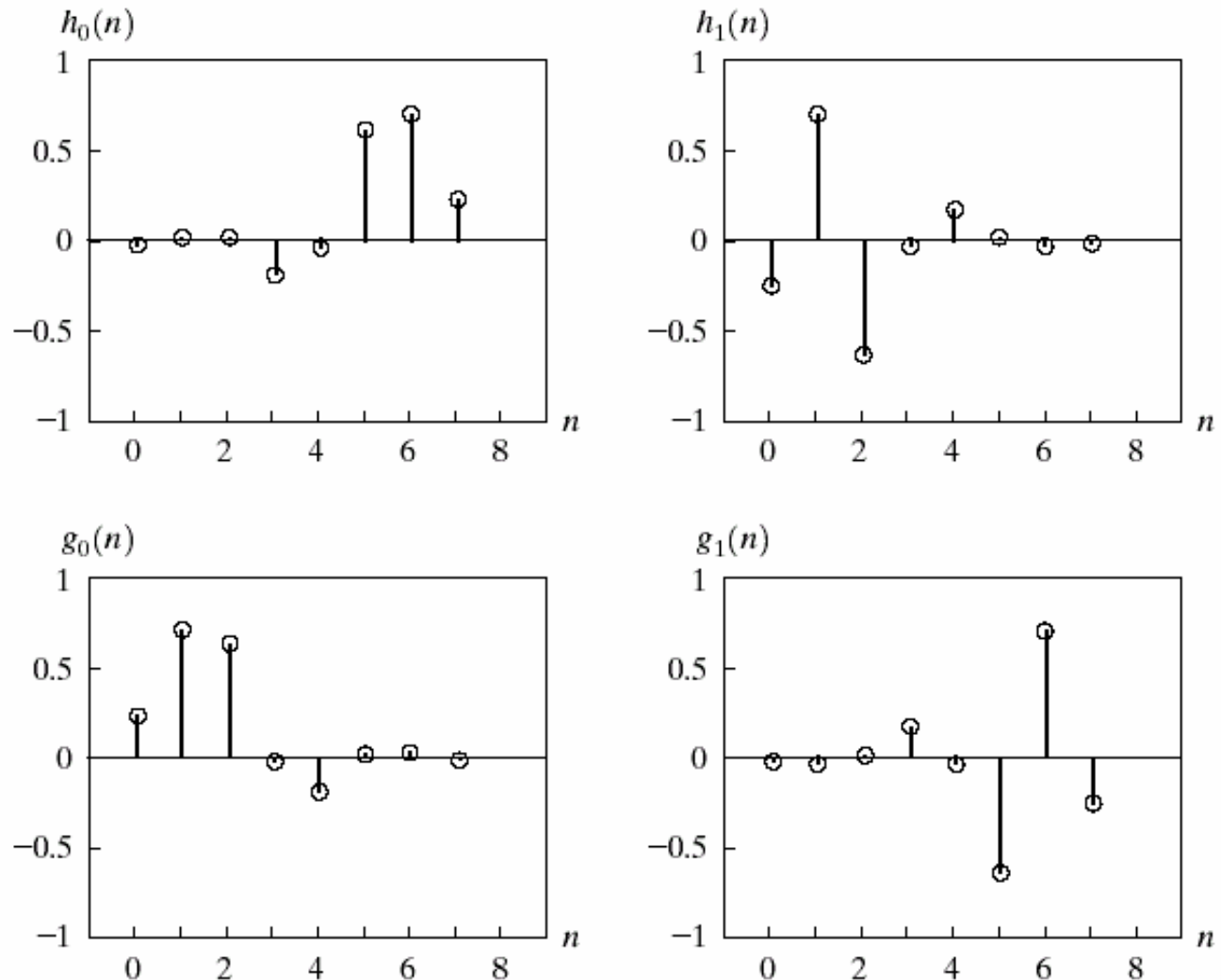


FIGURE 7.5 A two-dimensional, four-band filter bank for subband image coding.

7.1 Background-Subband Coding

FIGURE 7.6 The impulse responses of four 8-tap Daubechies orthonormal filters.



They satisfy perfect reconstruction and (7.21) and (7.22)

7.1 Background-Subband Coding

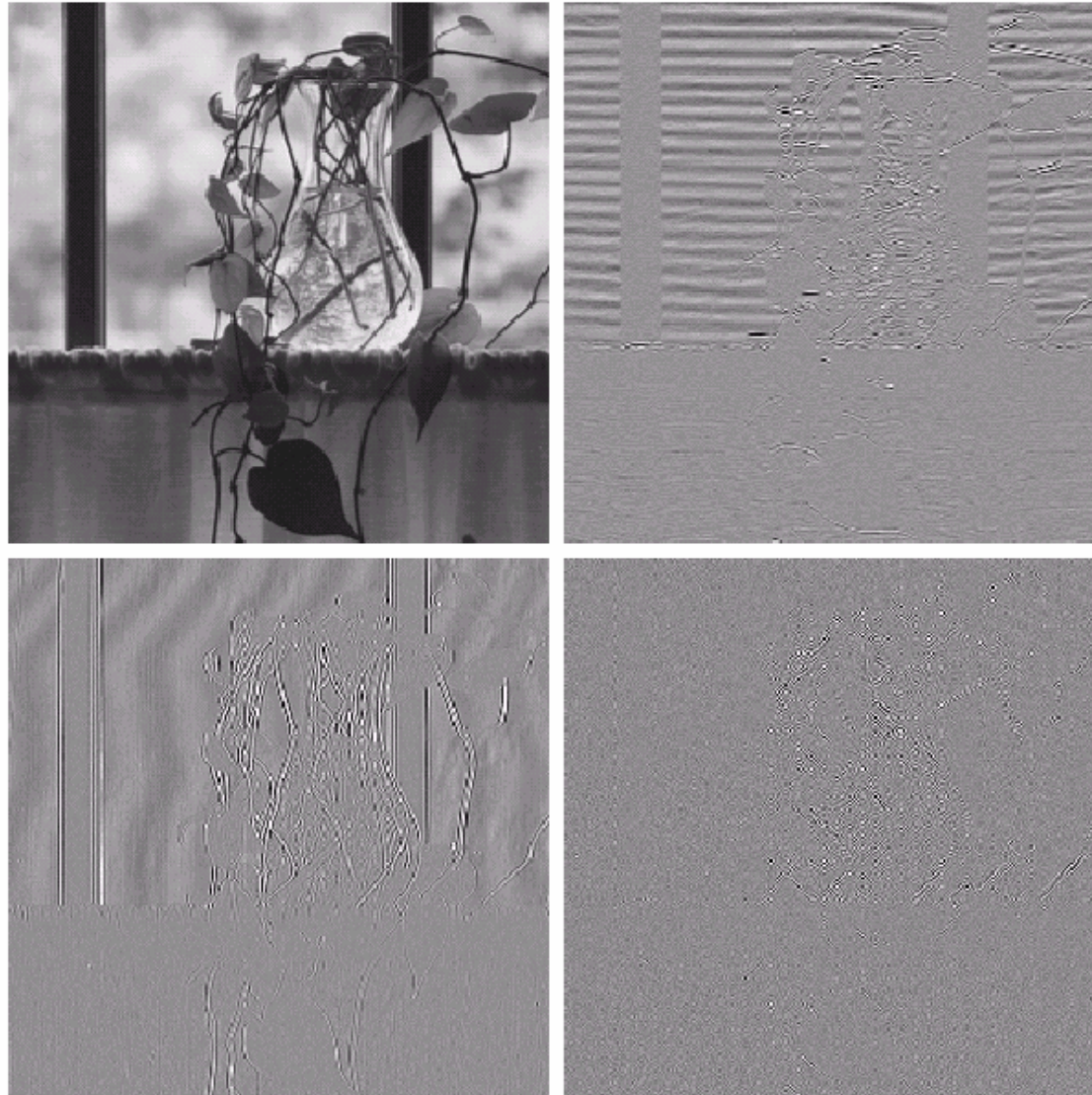
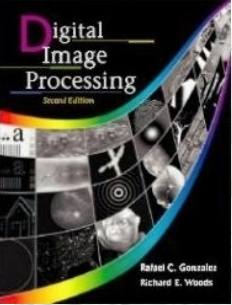


FIGURE 7.7 A four-band split of the vase in Fig. 7.1 using the subband coding system of Fig. 7.5.



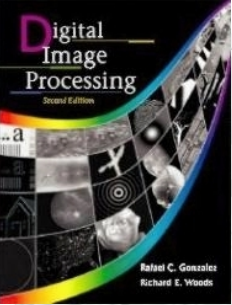
7.1 Background-Harr Transform

- The oldest and simplest known orthonormal wavelets
- The Harr transform is both separable and symmetric as

$$\mathbf{T}=\mathbf{H}\mathbf{F}\mathbf{H}$$

where \mathbf{F} is $N \times N$ image matrix and \mathbf{H} is $N \times N$ transform matrix and \mathbf{T} is the resulting $N \times N$ transform.

- For Harr transform, the transformation matrix \mathbf{H} contains the Harr basis function $h_k(z)$ defined over the continuous closed interval $[0,1]$ for $k=0,1,\dots,N-1$ where $N=2^n$.



7.1 Background-Harr Transform

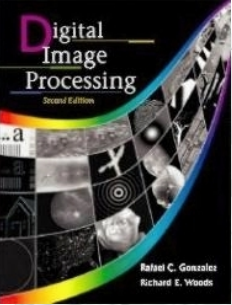
- To generate \mathbf{H} , we define $k=2^p + q-1$ where $0 \leq p \leq n-1$, $q=0$ or 1 for $p=0$, and $1 \leq q \leq 2^p$ for $p \neq 0$

- The Harr basis functions are

$$h_0(z) = h_{00}(z) = 1/N^{1/2}, \quad z \in [0, 1]$$

and

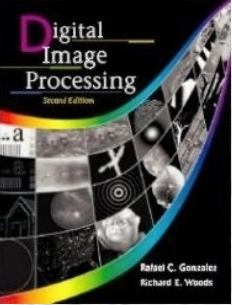
$$h_k(z) = h_{pq}(z) = \frac{1}{\sqrt{N}} \begin{cases} 2^{p/2} & (q-1)/2^p \leq z < (q-0.5)/2^p \\ -2^{p/2} & (q-0.5)/2^p \leq z < q/2^p \\ 0 & \text{otherwise, } z \in [0, 1] \end{cases}$$



7.1 Background-Harr Transform

- The i th row of an $N \times N$ Harr transformation matrix contains the elements of $h_i(z)$, $z=0/N, 1/N, \dots, (N-1)/N$
- If $N=4$, k , q , and p are assumed as the following values:

k	p	q
0	0	0
1	0	1
2	1	1
3	1	2



7.1 Background-Harr Transform

- The 4×4 transformation matrix is

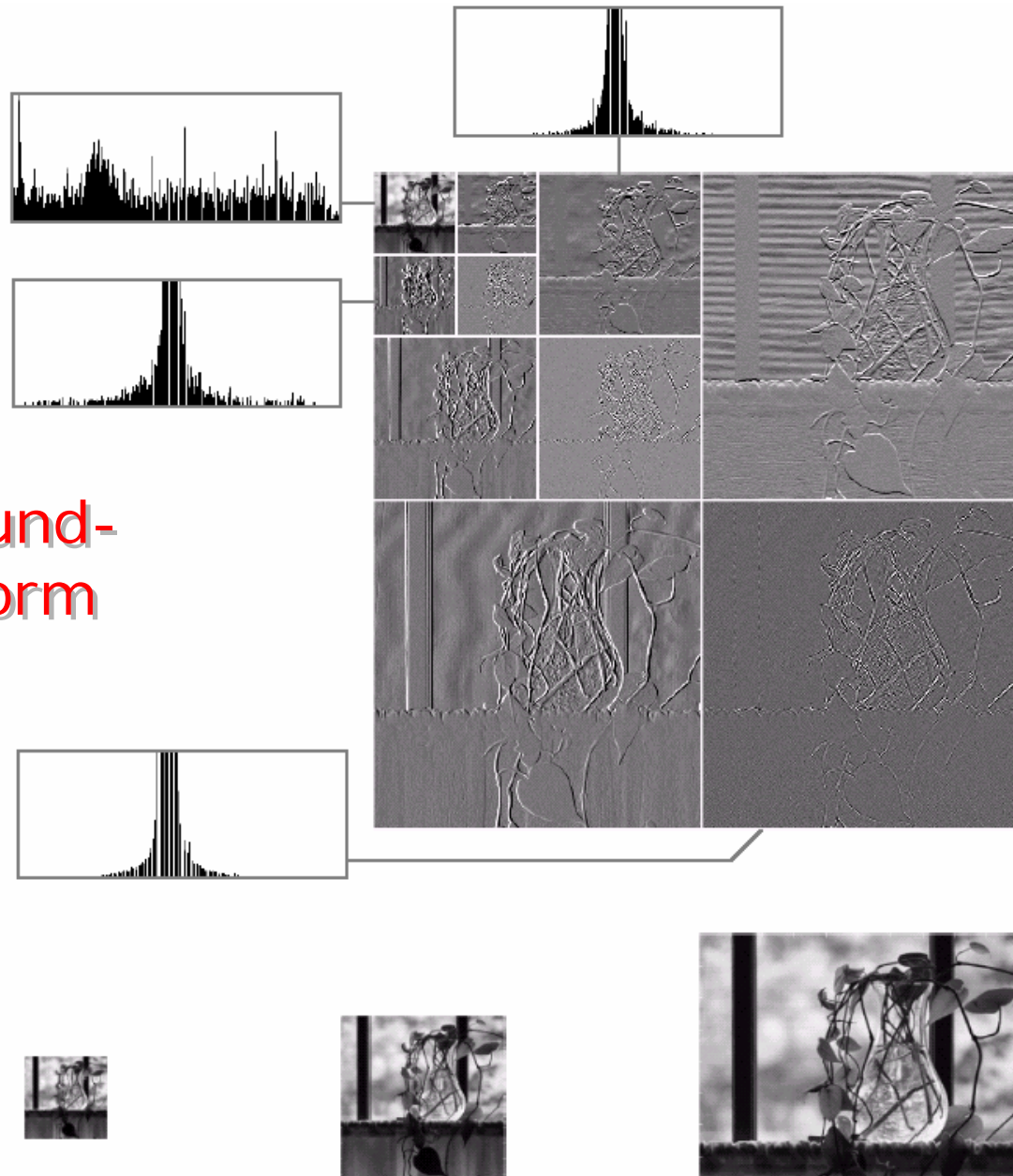
$$H_4 = \frac{1}{\sqrt{4}} \begin{bmatrix} 1 & 1 & 1 & 1 \\ 2 & 1 & -1 & -1 \\ \sqrt{2} & -\sqrt{2} & 0 & 0 \\ 0 & 0 & \sqrt{2} & -\sqrt{2} \end{bmatrix}$$

- The 2×2 transformation matrix is

$$H_2 = \frac{1}{\sqrt{2}} \begin{bmatrix} 1 & 1 \\ 1 & -1 \end{bmatrix}$$

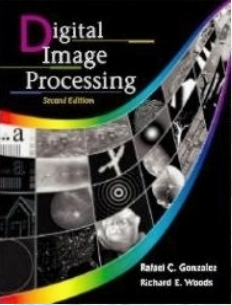
- The basis functions satisfy the QMF prototype filter in Table 7.1, the $h_0(n)$ and $h_1(n)$ are the elements of the first and the second rows of \mathbf{H}_2 .

7.1 Background-Harr Transform



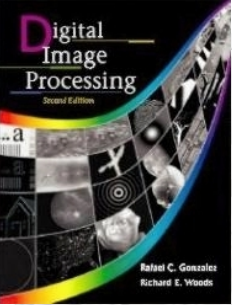
a
b c d

FIGURE 7.8 (a) A discrete wavelet transform using Haar basis functions. Its local histogram variations are also shown; (b)–(d) Several different approximations (64×64 , 128×128 , and 256×256) that can be obtained from (a).



7.2 Multiresolution Expansions

- ***Multi-resolution analysis*** (MRA)
- A ***scaling function*** is used to create a series of approximations of a function or image, each different by a factor of 2 from its neighboring approximation
- Additional functions, called ***wavelet***, are used to encode the difference between two adjacent approximation.



7.2 Multiresolution Expansions

- *Series expansion*

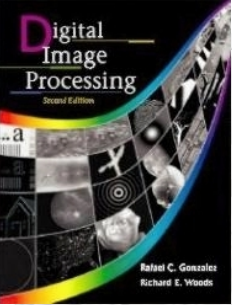
- A signal $f(x)$ can be represented as a linear combination of expansion functions as

$$f(x) = \sum_k \alpha_k \varphi_k(x)$$

- The expressible functions form a function space that is the closed span of the expansion set denoted as

$$V = \overline{\text{Span}\{\varphi_k(x)\}_k}$$

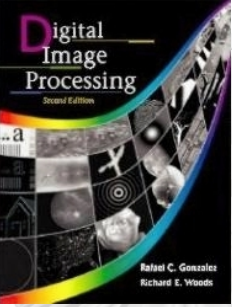
- $f(x) \in V$ means that $f(x)$ is in the closed span of $\{\varphi_k(x)\}$



7.2 Multiresolution Expansions

- For any function space V and the corresponding expansion set $\{\varphi_k(x)\}$ there is a set of dual functions denoted as $\{\tilde{\varphi}_k(x)\}$ that can be used to compute the α_k as

$$\alpha_k = \langle \tilde{\varphi}_k(x) \quad f(x) \rangle = \int \tilde{\varphi}_k^*(x) f(x) dx$$



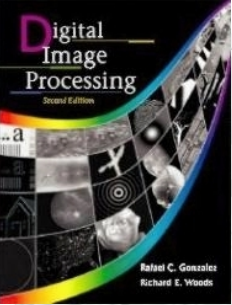
7.2 Multiresolution Expansions

- *Case 1:* The expansion functions form orthonormal basis for V that $\langle \varphi_j(x) \quad \varphi_k(x) \rangle = \delta_{jk}$
- The basis and its dual are equivalent $\varphi_k(x) = \tilde{\varphi}_k(x)$
- and then $\alpha_k = \langle \varphi_k(x) \quad f(x) \rangle$
- *Case 2:* If the expansion functions are not orthonormal, but orthogonal basis for V then

$$\langle \varphi_j(x) \quad \varphi_k(x) \rangle = 0 \quad \text{if } j \neq k$$

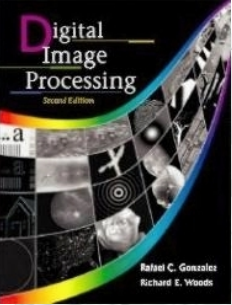
- and the basis functions and their duals are called bi-orthogonal.
- The biorthogonal basis and their duals are

$$\langle \varphi_j(x) \quad \tilde{\varphi}_k(x) \rangle = \delta_{jk}$$



7.2 Multiresolution Expansions

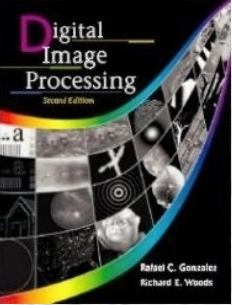
- *Case 3*: If the expansion set is not a basis for V , but support the expansion, then it is a spanning set in which there is more than one set of α_k for any $f(x) \in V$
- The expansions and their duals are said to be overcomplete or redundant. They form a frame in which
$$A\|f(x)\|^2 \leq \sum_k |\langle \varphi_k(x) \quad f(x) \rangle|^2 \leq B\|f(x)\|^2$$
- A and B “frame” the normalized inner products of the expansion coefficients and the function.



7.2 Multiresolution Expansions

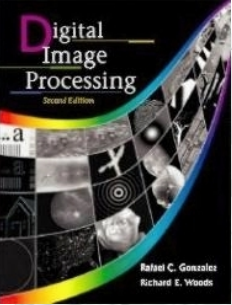
- If $A=B$ the expansion is called a *tight frame*, and it can be shown that

$$f(x) = \frac{1}{A} \sum_k \langle \varphi_k(x) | f(x) \rangle \varphi_k(x)$$



7.2 Multiresolution Expansions

- *Scaling Functions*
- Consider a set of expansion functions composed of integer translations and binary scaling of the real square-integrable function $\varphi(x)$, that is the set $\{\varphi_{j,k}(x)\}$ where $\varphi_{j,k}(x) = 2^{j/2} \varphi(2^j x - k)$
- For all $j, k \in I$ and $\varphi(x) \in L^2(\mathbb{R})$
- j determines the position of $\varphi_{j,k}(x)$, and k determines the width of $\varphi_{j,k}(x)$
- $\varphi_{j,k}(x)$ is called the scaling function



7.2 Multiresolution Expansions

- If we restrict j to a specific value $j=j_0$ then $\{\varphi_{j_0,k}(x)\}$ is a subset of $\{\varphi_{j,k}(x)\}$

and

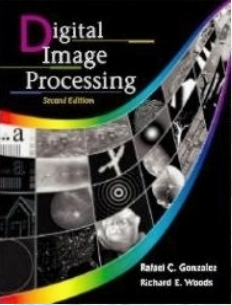
$$f(x) = \sum_k \alpha_k \varphi_{j,k}(x) \quad V_j = \overline{\text{Span}\{\varphi_{j,k}(x)\}}$$

- *Figure 7.9*

$$f(x) = 0.5\varphi_{1,0}(x) + \varphi_{1,1}(x) - 0.25\varphi_{1,4}(x)$$

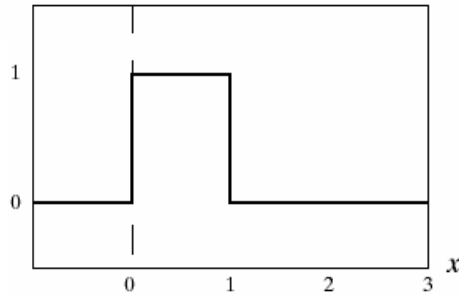
- *Expansion function can be decomposed as*

$$\varphi_{0,k}(x) = 1/2^{0.5} \varphi_{1,2k}(x) + 1/2^{0.5} \varphi_{1,2k}(x)$$

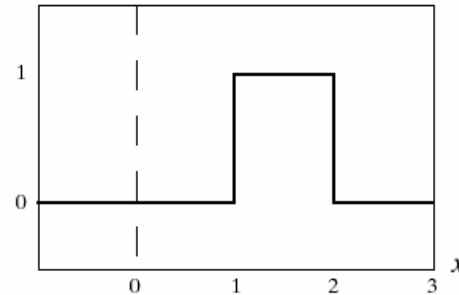


7.2 Multiresolution Expansions

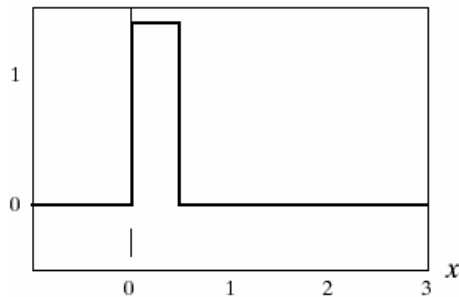
$$\varphi_{0,0}(x) = \varphi(x)$$



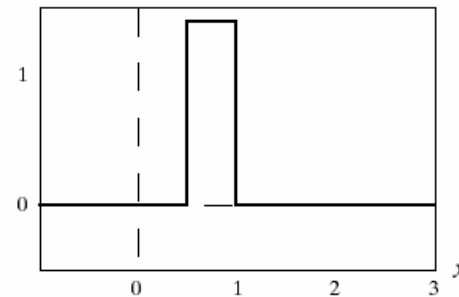
$$\varphi_{0,1}(x) = \varphi(x - 1)$$



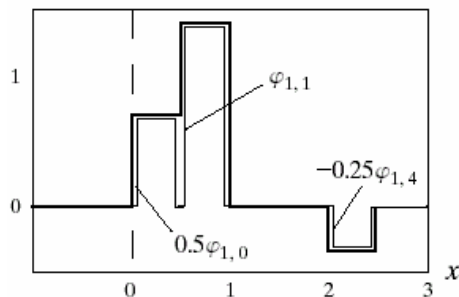
$$\varphi_{1,0}(x) = \sqrt{2} \varphi(2x)$$



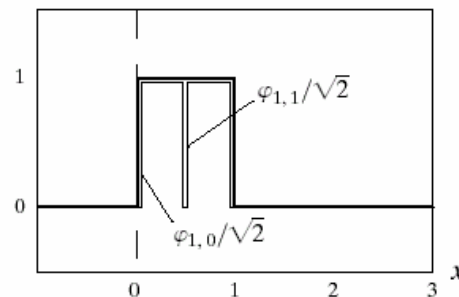
$$\varphi_{1,1}(x) = \sqrt{2} \varphi(2x - 1)$$



$$f(x) \in V_1$$

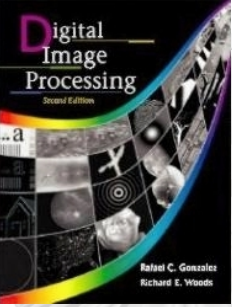


$$\varphi_{0,0}(x) \in V_1$$



a b
c d
e f

FIGURE 7.9 Haar scaling functions in V_0 in V_1 .

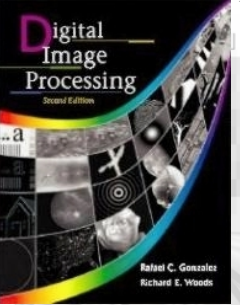


7.2 Multiresolution Expansions

- ***Four requirements for MRA***
- MRA requirement 1: *The scaling function is orthogonal to its integer translates*
- MRA requirement 2: *The subspace spanned by the scaling function at low scales are nested within those spanned at higher scales.*
- *Subspaces containing high resolution function must also contain all lower resolution functions*

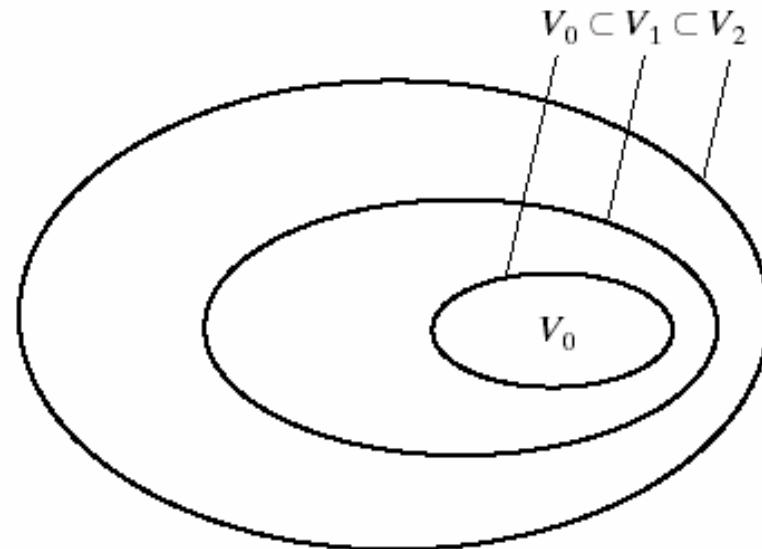
$$V_{-\infty} \subset \dots \subset V_{-1} \subset V_0 \subset V_1 \subset V_2 \dots \subset V_{\infty}$$

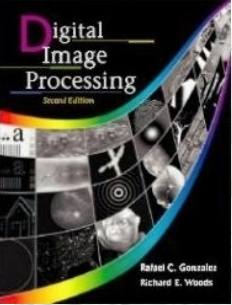
- *If $f(x) \in V_j$ then $f(2x) \in V_{j+1}$*



7.2 Multiresolution Expansions

FIGURE 7.10 The nested function spaces spanned by a scaling function.





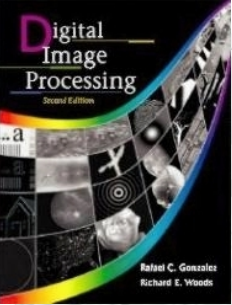
7.2 Multiresolution Expansions

- MRA requirement 3: *The only function that is common to all V_j is $f(x)=0$*
- MRA requirement 4: *Any function can be represented with arbitrary precision.*
- All measurable square-integrable functions can be represented in the limit as $j \rightarrow \infty$ as

$$V_{\infty} = \{L^2(\mathbf{r})\}$$

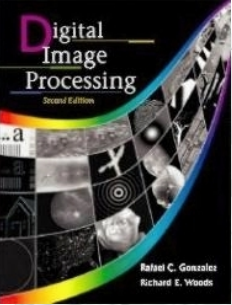
- The expansion function of subspace V_j can be expressed as a weighted sum of expansion functions in V_{j+1} space as

$$\varphi_{j,k}(x) = \sum_n \alpha_n \varphi_{j+1,n}(x)$$



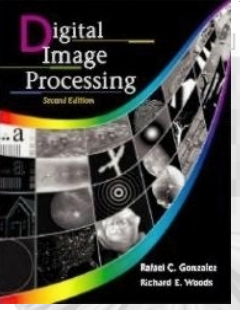
7.2 Multiresolution Expansions

- Change α_n to $h_\varphi(n)$
$$\varphi_{j,k}(x) = \sum_n h_\varphi(n) 2^{(j+1)/2} \varphi(2^{(j+1)/2} x - n)$$
- Set $j=k=0$ then $\varphi_{0,0}(x) = \varphi(x)$
$$\varphi(x) = \sum_n h_\varphi(n) 2^{1/2} \varphi(2x - n)$$
- It is called *the refinement equation, MRA equation, or the dilation equation.*
- $h_\varphi(n)$ coefficients are called *scaling function coefficients.*
- h_φ is referred as *scaling vector*
- *The scaling function for Harr function are $h_\varphi(0) = h_\varphi(1) = 1/2^{1/2}$ then*
$$\varphi(x) = 1/2^{1/2} [2^{1/2} \varphi(2x) + 2^{1/2} \varphi(2x-1)]$$
$$= \varphi(2x) + \varphi(2x-1)$$



7.2 Multiresolution Expansions

- *Wavelet functions*
- *We define the set $\{\psi_{j,k}(x)\}$ as*
$$\psi_{j,k}(x) = 2^{j/2} \psi(2^j x - k)$$
- *The W_j space is*
$$W_j = \overline{\text{Span}_k \{\psi_{j,k}(x)\}}$$
- *If $f(x) \in W_j$ then $f(x) = \sum_k \alpha_k \psi_{j,k}(x)$*



7.2 Multiresolution Expansions

$$V_2 = V_1 \oplus W_1 = V_0 \oplus W_0 \oplus W_1$$

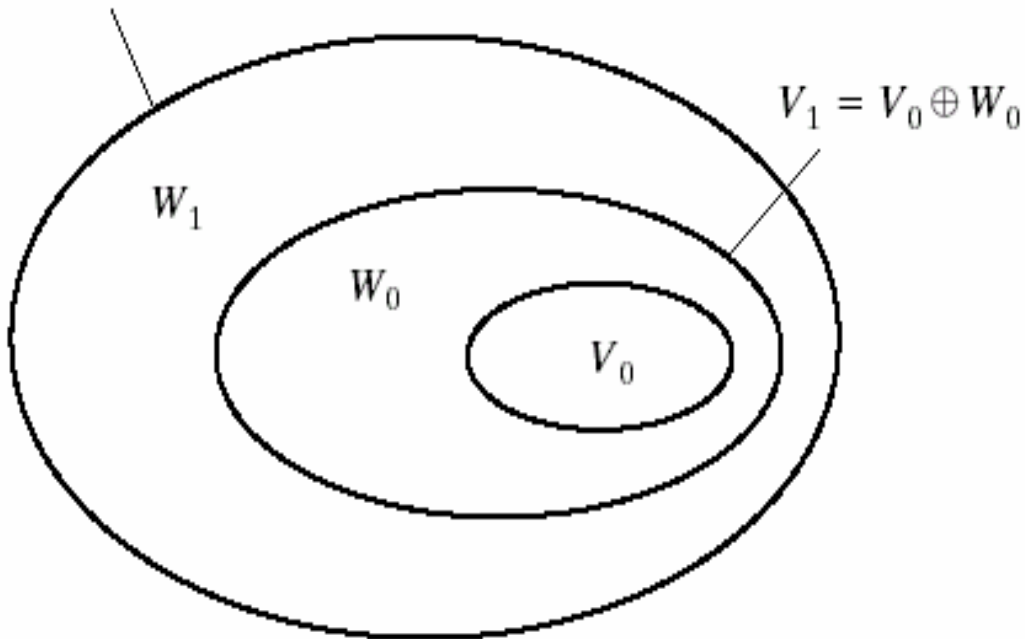
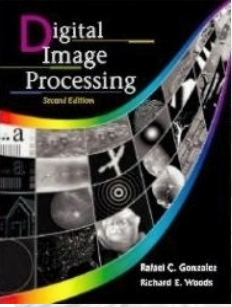
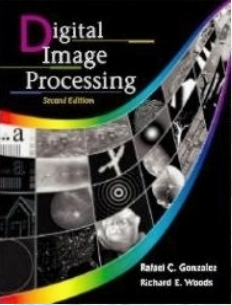


FIGURE 7.11 The relationship between scaling and wavelet function spaces.



7.2 Multiresolution Expansions

- The scaling and wavelet subspaces in Figure 7.11 are related as $V_{j+1} = V_j \oplus W_j$ where \oplus denotes the unions of spaces.
- The orthogonal complement of V_j in V_{j+1} is W_j and all members of V_j are orthogonal to the member of W_j ,
Thus
- $\langle \varphi_{j,k}(x) \psi_{j,k}(x) \rangle = 0$ for all appropriate $j, k, l \in \mathbf{Z}$
- We can express the space of all measurable square-integrable functions as
- $L^2(\mathbf{R}) = V_0 \oplus W_0 \oplus W_1 \oplus \dots$ or $L^2(\mathbf{R}) = V_1 \oplus W_1 \oplus W_2 \oplus \dots$
- Or $L^2(\mathbf{R}) = \dots \oplus W_{-1} \oplus W_0 \oplus W_1 \oplus \dots$



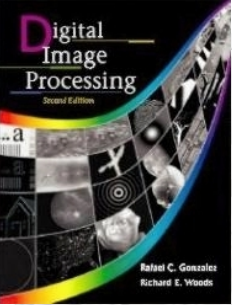
7.2 Multiresolution Expansions

- If $f(x)$ is an element of V_1 , but not V_0 , an expansion of $f(x)$ using V_0 scaling function; wavelet from W_0 would encode the difference between the approximation and the actual function. It can be generalized as

$$L^2(\mathbf{R}) = V_{j_0} \oplus W_{j_0} \oplus W_{j_0+1} \oplus \dots$$

where j_0 is an arbitrary starting scale

- Any wavelet function can be expressed as a weighted sum of shifted double-resolution scaling functions that is $\psi(x) = \sum_n h_\psi(n) 2^{1/2} \phi(2x-n)$
- *Where $h_\psi(n)$ is wavelet function coefficients and h_ψ is the wavelet vector.*



7.2 Multiresolution Expansions

- $h_{\psi}(n)$ is related to $h_{\phi}(n)$ as

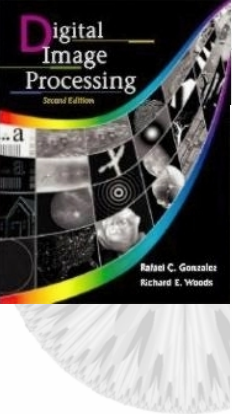
$$h_{\psi}(n) = (-1)^n h_{\phi}(1-n)$$

- The Harr scaling factor illustrated as $h_{\phi}(0) = h_{\phi}(1) = 1/2^{1/2}$

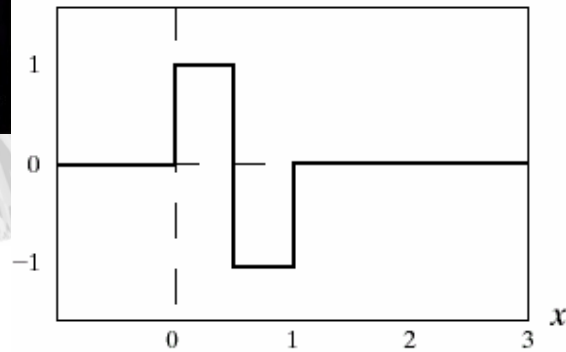
$$h_{\psi}(0) = (-1)^0 h_{\phi}(1-0) = 1/2^{1/2}$$

$$h_{\psi}(1) = (-1)^1 h_{\phi}(1-1) = -1/2^{1/2}$$

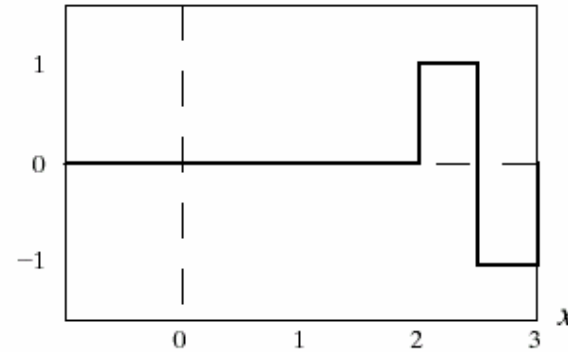
- We get $\psi(x) = \phi(2x) - \phi(2x-1)$
The Harr wavelet function is
$$\psi(x) = \begin{cases} 1 & 0 \leq x < 0.5 \\ -1 & 0.5 \leq x < 1 \\ 0 & \text{elsewhere} \end{cases}$$



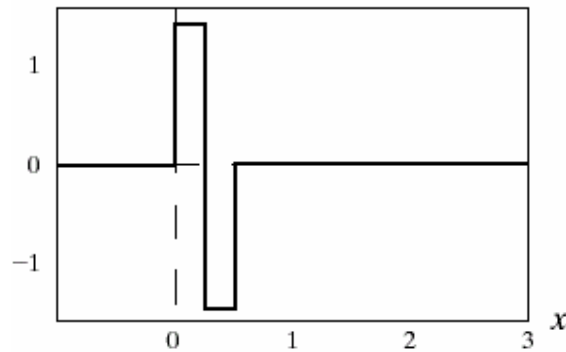
$$\psi(x) = \psi_{0,0}(x)$$



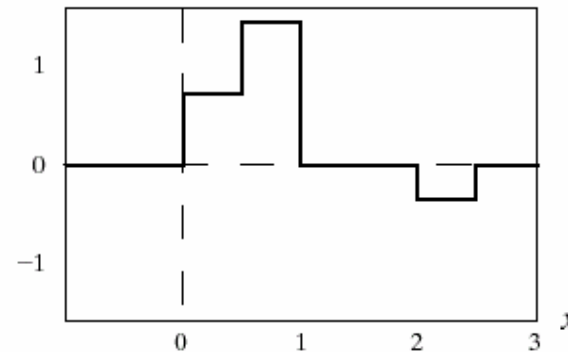
$$\psi_{0,2}(x) = \psi(x - 2)$$



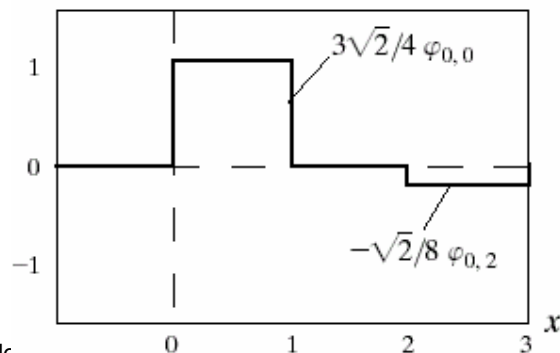
$$\psi_{1,0}(x) = \sqrt{2} \psi(2x)$$



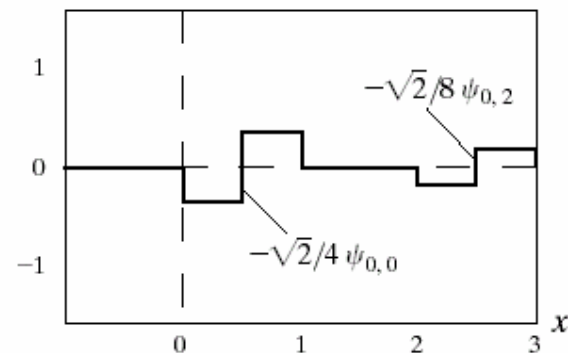
$$f(x) \in V_1 = V_0 \oplus W_0$$



$$f_a(x) \in V_0$$



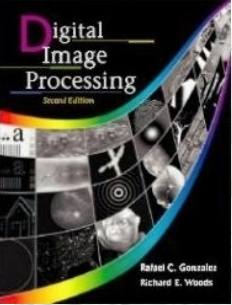
$$f_d(x) \in W_0$$



a	b
c	d
e	f

FIGURE 7.12 Haar wavelet functions in W_0 and W_1 .

7.2 Multiresolution Expansions



7.2 Multiresolution Expansions

- A function in V_1 that is not subspace in V_0 can be expanded using V_0 and W_0 as

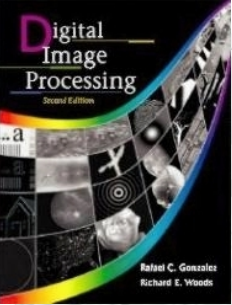
$$f(x) = f_a(x) + f_d(x)$$

where

$$f_a(x) = \frac{3\sqrt{2}}{4} \varphi_{0,0}(x) - \frac{\sqrt{2}}{8} \varphi_{0,2}(x)$$

$$f_d(x) = \frac{-\sqrt{2}}{4} \psi_{0,0}(x) - \frac{\sqrt{2}}{8} \psi_{0,2}(x)$$

$f_a(x)$ is an approximation of $f(x)$ using V_0 scaling function, whereas $f_d(x)$ is the difference $f(x) - f_a(x)$ as a sum of W_0 wavelets



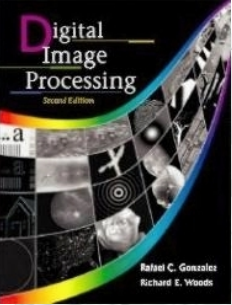
7.3 Wavelets transform in one dimension- the wavelet series expansion

- Expand $f(x)$ related to wavelet $\psi(x)$ and scaling function $\varphi(x)$ as

$$f(x) = \sum_k c_0(k) \varphi_{0,k}(x) + \sum_{j=j_0}^{\infty} \sum_k d_j(k) \psi_{j,k}(x)$$

- Where j_0 is an arbitrary starting scale and $c_{j_0}(k)$'s and $d(k)$ are relabeled α . The $c_{j_0}(k)$'s are normally called the approximation or scaling coefficients and the $d_j(k)$'s are referred as the detail or wavelet coefficients

- $$c_0(k) = \langle f(x) \quad \varphi_{0,k}(x) \rangle = \int f(x) \varphi_{0,k}(x) dx$$
$$d_j(k) = \langle f(x) \quad \psi_{j,k}(x) \rangle = \int f(x) \psi_{j,k}(x) dx$$



7.3 Wavelets transform in one dimension

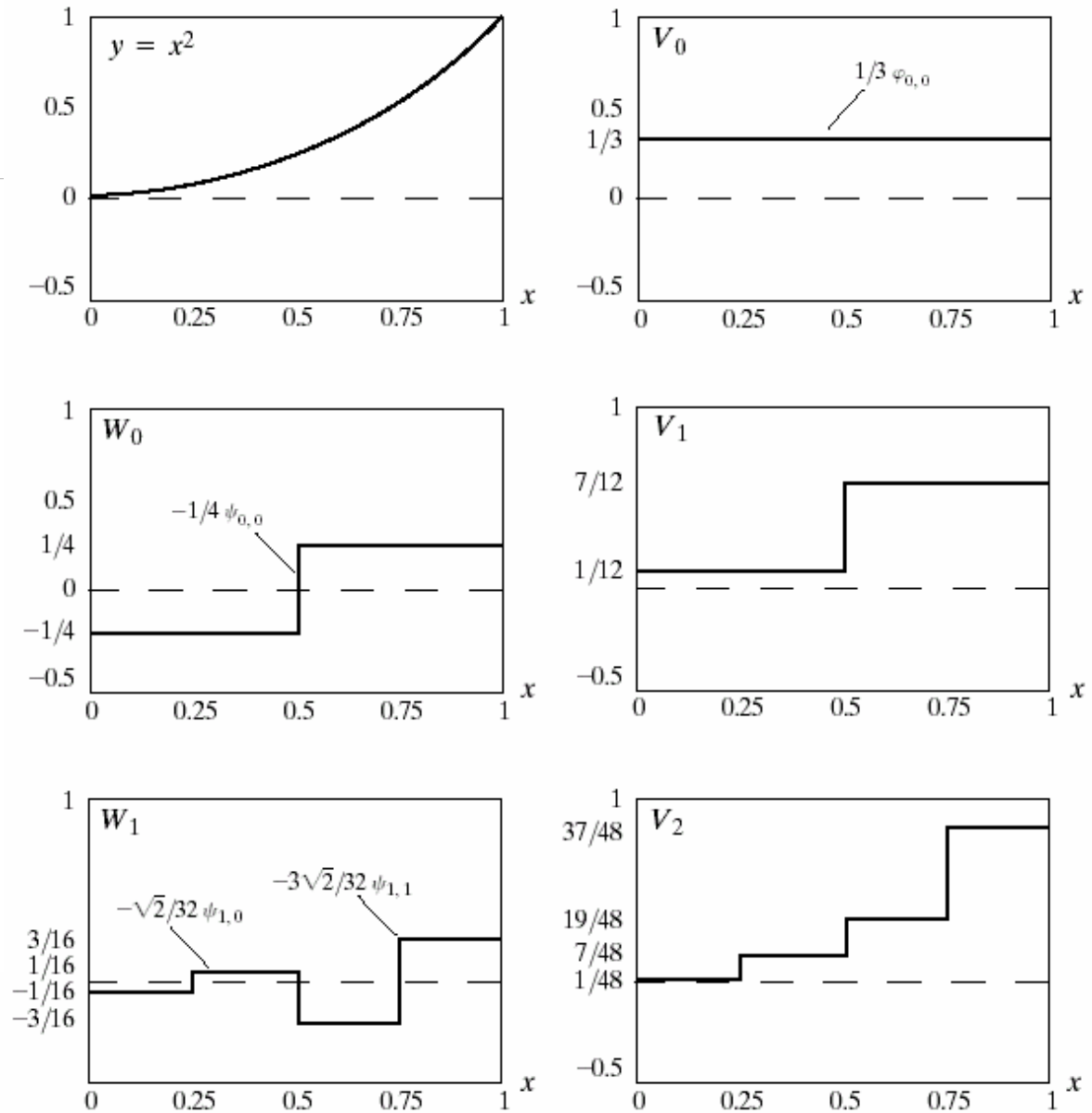
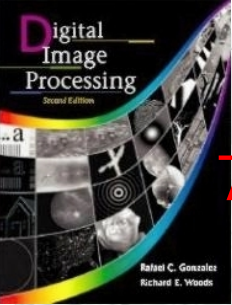


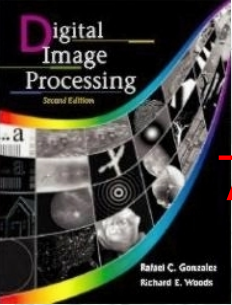
FIGURE 7.13 A wavelet series expansion of $y = x^2$ using Haar wavelets.



7.3 Wavelets transform in one dimension- the wavelet series expansion

- Wavelet series expansion

$$y = \underbrace{\frac{1}{3} \varphi_{00}(x)}_{V_0} + \underbrace{\left[-\frac{1}{4} \psi_{00}(x) \right]}_{W_0} + \underbrace{\left[-\frac{\sqrt{2}}{32} \psi_{10}(x) - \frac{3\sqrt{2}}{32} \psi_{11}(x) \right]}_{W_1} + \dots$$



7.3 Wavelets transform in one dimension- the discrete wavelet transform

- For discrete case, the series expansion becomes

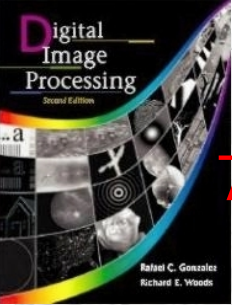
$$W_{\varphi}(j_0, k) = \frac{1}{\sqrt{M}} \sum_x f(x) \varphi_{j_0, k}(x)$$

for $j \geq j_0$

$$W_{\psi}(j, k) = \frac{1}{\sqrt{M}} \sum_x f(x) \psi_{j, k}(x)$$

$$f(x) = \frac{1}{\sqrt{M}} \sum_x W_{\varphi}(j_0, k) \varphi_{j_0, k}(x) + \frac{1}{\sqrt{M}} \sum_{j=j_0}^{\infty} \sum_x W_{\psi}(j, k) \psi_{j_0, k}(x)$$

- Here $f(x)$, $\varphi_{j_0, k}(x)$, $\psi_{j, k}(x)$ are functions of the discrete variable $x=0, 1, 2, \dots, M-1$
- For example $f(x) = f(x_0 + x\Delta x)$ for some x_0 , Δx , and $x=0, 1, 2, \dots, M-1$.
- Normally, we select $M=2^J$, $j=0, 1, 2, \dots, J-1$, $k=0, 1, \dots, 2^j-1$

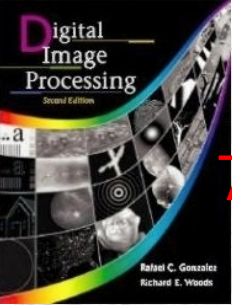


7.3 Wavelets transform in one dimension- the discrete wavelet transform

- **Example 7.8**
- $f(0)=1, f(1)=4, f(2)=-3, f(3)=0, M=4, J=2$, and with $j_0=0$, the summation is performed over $x=0,1,2,3, j=0,1$, and $k=0$ for $j=0$ or $k=0, 1$ for $j=1$.
- Using Harr scaling and wavelet functions (the rows of \mathbf{H}_4) and assume that four samples of $f(x)$ are distributed over the support of basis functions.

$$W_{\varphi}(0,0) = \frac{1}{2} \sum_x f(x) \varphi_{0,0}(x) = \frac{1}{2} [1 \times 1 + 4 \times 1 - 3 \times 1 + 0 \times 1] = 1$$

$$W_{\psi}(0,0) = \frac{1}{2} \sum_x f(x) \psi_{0,0}(x) = \frac{1}{2} [1 \times 1 + 4 \times 1 - 3 \times (-1) + 0 \times (-1)] = 4$$

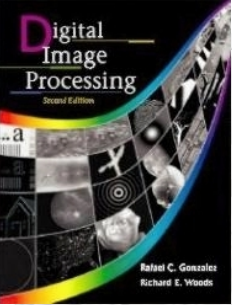


7.3 Wavelets transform in one dimension- the discrete wavelet transform

$$W_{\psi}(1,0) = \frac{1}{2} \sum_x f(x) \psi_{1,0}(x) = -1.5\sqrt{2}$$

$$W_{\psi}(1,1) = \frac{1}{2} \sum_x f(x) \psi_{1,1}(x) = -1.5\sqrt{2}$$

$$f(x) = \frac{1}{2} W_{\varphi}(0,0) \varphi_{0,0}(x) + W_{\psi}(0,1) \psi_{0,1}(x) \\ + W_{\psi}(1,0) \psi_{1,0}(x) + W_{\psi}(1,1) \psi_{1,1}(x)$$



7.3 Wavelets transform in one dimension- the continuous wavelet transform

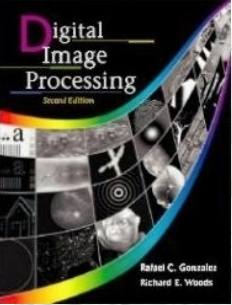
- CWT: transform a continuous function into a highly redundant function of two continuous variables - translation and scale

$$W_{\psi}(s, \tau) = \int_{-\infty}^{\infty} f(x) \psi_{s, \tau}(x) dx$$

where

$$\psi_{s, \tau}(x) = \frac{1}{\sqrt{s}} \psi\left(\frac{x - \tau}{s}\right)$$

s and τ are called the scale and translation parameters.



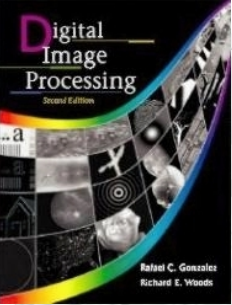
7.3 Wavelets transform in one dimension- the continuous wavelet transform

- ICWT

$$f(x) = \frac{1}{C_\psi} \int_0^\infty \int_{-\infty}^\infty W_\psi(s, \tau) \frac{\psi_{s,\tau}(x)}{s^2} d\tau ds$$

where

$$C_\psi = \int_{-\infty}^\infty \frac{|\Psi(u)|^2}{u} du$$



7.3 Wavelets transform in one dimension- the continuous wavelet transform

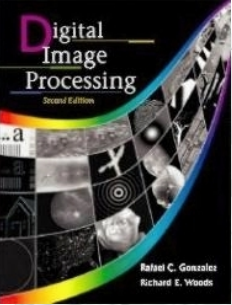
- The Mexican hat wavelet

$$\psi(x) = ((2/3^{1/2})\pi^{1/4})(1-x^2)e^{-x^2/2}$$

Figure 7.14(a) $f(x) = \psi_{1,10}(x) + \psi_{6,80}(x)$

Figure 7.14(c) shows a portion ($1 \leq s \leq 10$ and $\tau \leq 100$) of the CWT of Figure 7.14(a)

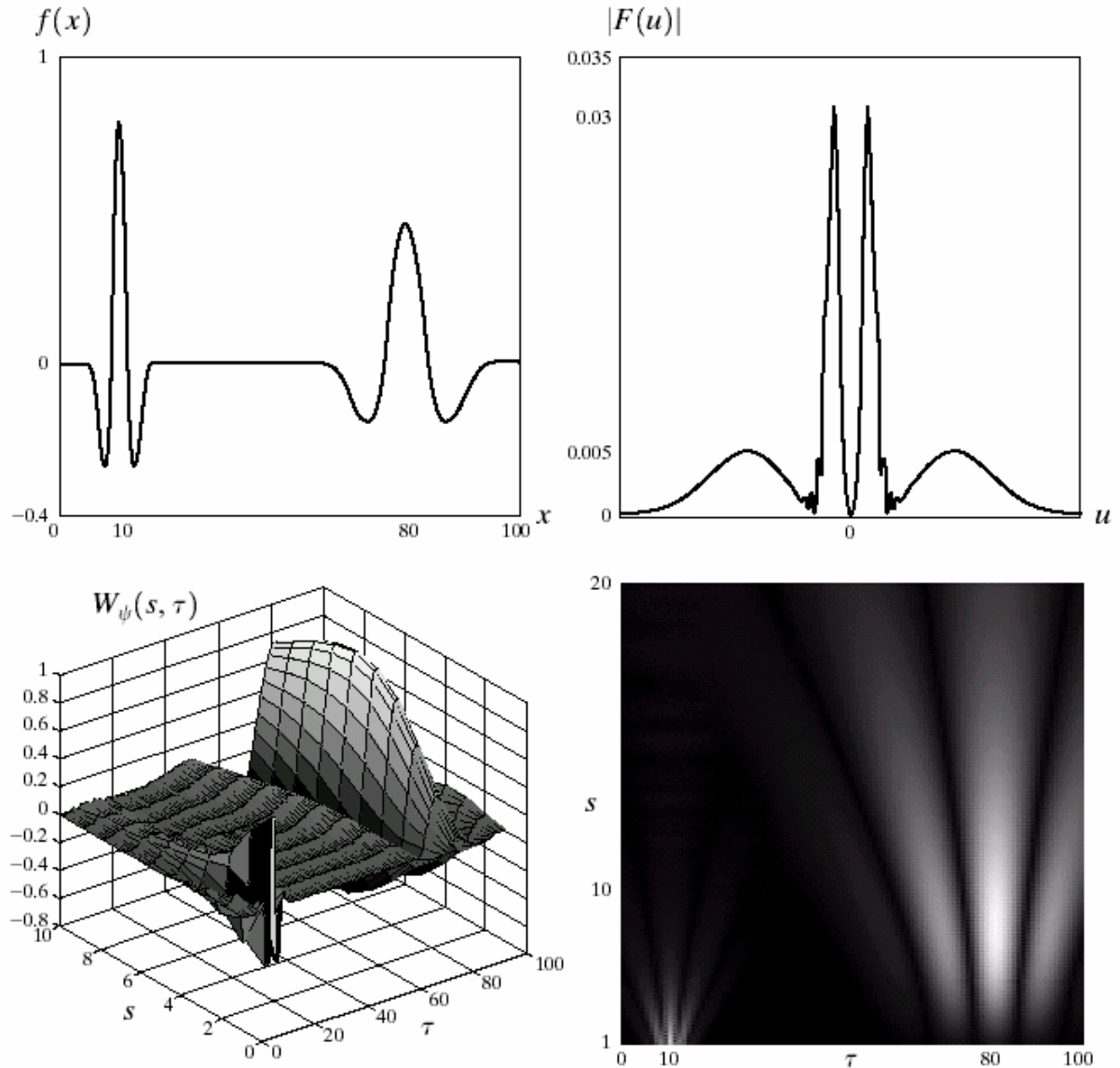
- *Continuous translation τ*
- *Continuous scaling s*
- *The set of transformation coefficients $\{W_{\psi}(s, \tau)\}$ and basis functions $\{\psi_{s, \tau}(x)\}$ are infinite.*

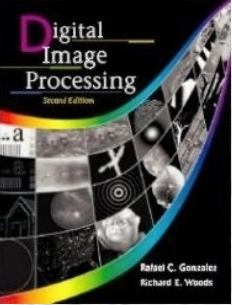


7.3 Wavelets transform in one dimension

a b
c d

FIGURE 7.14 The continuous wavelet transform (c and d) and Fourier spectrum (b) of a continuous one-dimensional function (a).



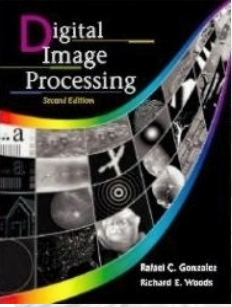


7.4 Fast Wavelet Transform (FWT)

- *FWT* exploits a surprising but fortunate relationship between the coefficients of the *DWT* at adjacent scales (*known as Herringbone algorithm*)
- *Consider the multi-resolution refinement equation:*
$$\varphi(x) = \sum_n h_\varphi(n) 2^{1/2} \varphi(2x-n)$$
- *Scaling x by 2, translating by k , and letting $m=2k+n$ then*

$$\begin{aligned}\varphi(2^j x - k) &= \sum_n h_\varphi(n) 2^{1/2} \varphi(2(2^j x - k) - n) \\ &= \sum_n h_\varphi(m - 2k) 2^{1/2} \varphi(2^{j+1} x - m)\end{aligned}$$

- *h_φ can be thought of as the “weights” used to expand $\varphi(2^j x - k)$ as sum of the scale $j+1$ scaling function.*



7.4 Fast Wavelet Transform (FWT)

Similarly, for $\psi(2^j x - k)$ we have

$$\psi(2^j x - k) = \sum_n h_\psi(m - 2k) 2^{1/2} \psi(2^{j+1} x - m)$$

For DWT,

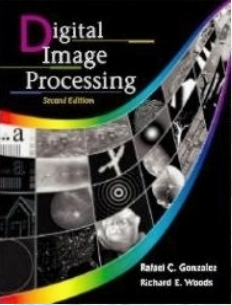
$$W_\psi(j, k) = \frac{1}{\sqrt{M}} \sum_x f(x) 2^{j/2} \psi(2^j x - k)$$

Replacing $\psi(2^j x - k)$, we have

$$W_\psi(j, k) = \frac{1}{\sqrt{M}} \sum_x f(x) 2^{j/2} \left[\sum_m h_\psi(m - 2k) \sqrt{2} \phi(2^{j+1} x - m) \right]$$

or

$$W_\psi(j, k) = \sum_m h_\psi(m - 2k) \left[\frac{1}{\sqrt{M}} \sum_x f(x) 2^{(j+1)/2} \sqrt{2} \phi(2^{j+1} x - m) \right]$$



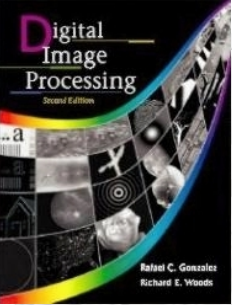
7.4 Fast Wavelet Transform (FWT)

- where the bracketed quantity is identical to the DWT transform pair with $j_0=j+1$, so

$$W_{\psi}(j, k) = \sum_m h_{\psi}(m - 2k) W_{\phi}(j+1, m)$$

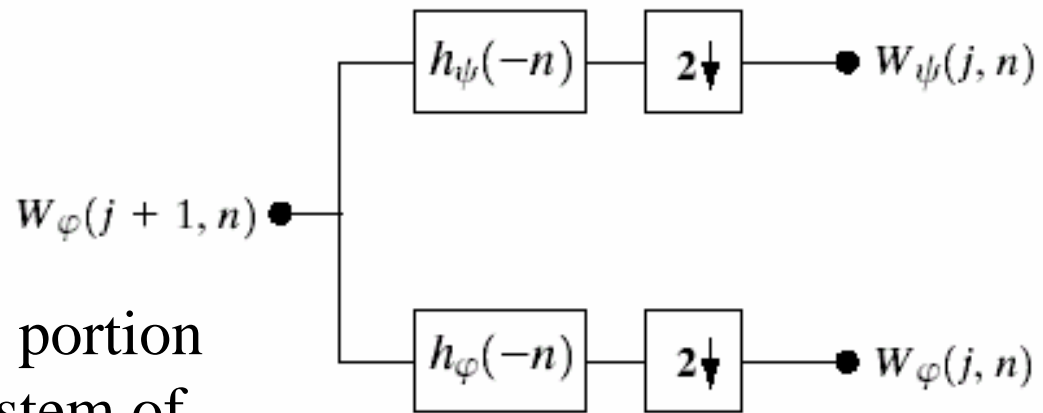
- The DWT detail coefficients at scale j are a function of the DWT approximation coefficients at scale $j+1$.
- Similarly, we have

$$W_{\phi}(j, k) = \sum_m h_{\phi}(m - 2k) W_{\psi}(j+1, m)$$



7.4 Fast Wavelet Transform

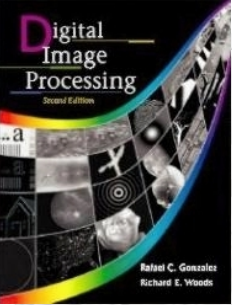
FIGURE 7.15 An FWT analysis bank.



It is identical to the analysis portion of the two-band subband system of Figure 7.4 with $h_0(n) = h_\varphi(-n)$ and $h_1(n) = h_\psi(-n)$

$$W_\psi(j, k) = h_\psi(-n) \otimes W_\psi(j+1, n) \Big|_{n=2k, k \geq 0}$$

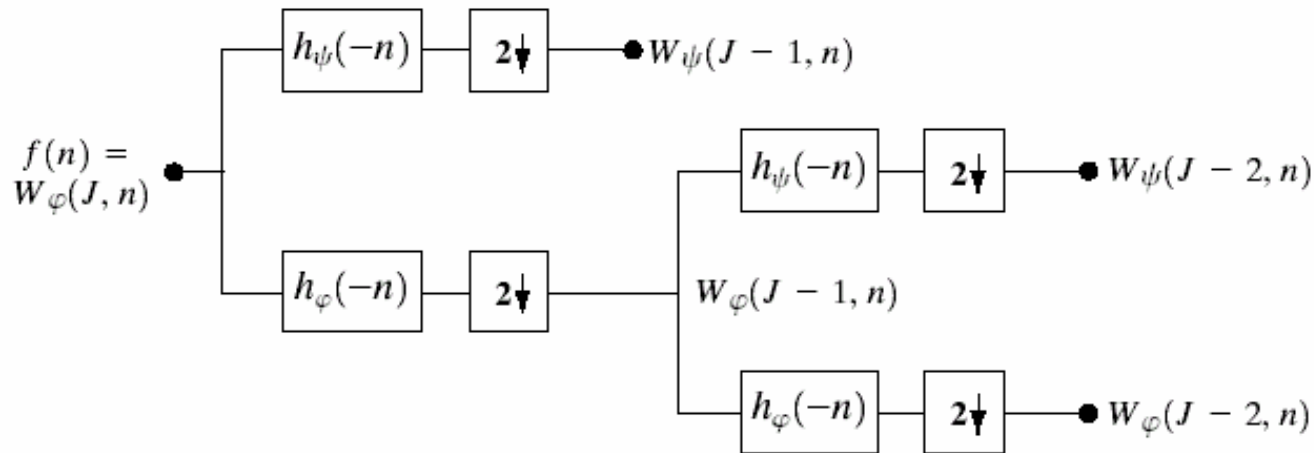
$$W_\varphi(j, k) = h_\varphi(-n) \otimes W_\psi(j+1, n) \Big|_{n=2k, k \geq 0}$$



7.4 Fast Wavelet Transform

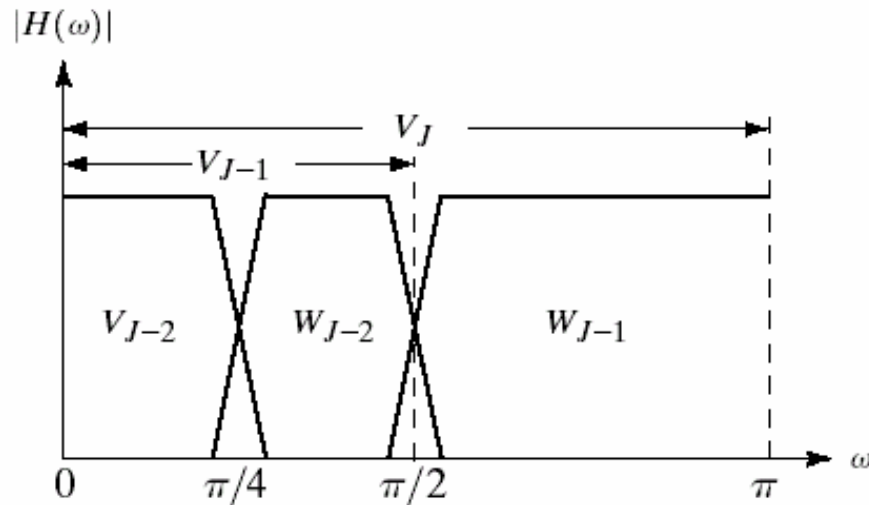
- Figure 7.16 shows a two-stage filterbank for generating the coefficients at two highest scales of the transform.
- The highest level is $W_\phi(J, n) = f(n)$, where J is the highest scale.
- $W_\phi(J-1, n)$ is the low-pass approximation component, and $W_\psi(J-1, n)$ is the high-pass detail component
- The second filter bank split the spectrum and the subspace V_{J-1} , the lower half-band, into quarter-band subspaces W_{J-2} , and V_{J-2} , with corresponding DWT coefficients: $W_\phi(J-2, n)$ and $W_\psi(J-2, n)$.

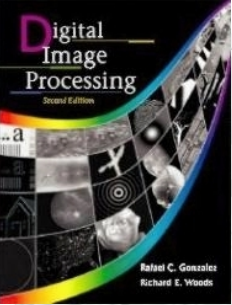
7.4 Fast Wavelet Transform



a
b

FIGURE 7.16
(a) A two-stage or two-scale FWT analysis bank and (b) its frequency splitting characteristics.



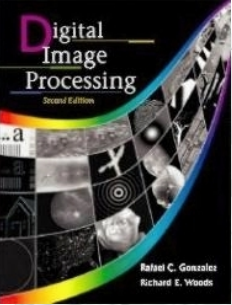


7.4 Fast Wavelet Transform

- Consider discrete function $f(n) = \{1, 4, -3, 0\}$
- The corresponding scaling and wavelet vectors

$$h_{\varphi}(n) = \begin{cases} 1/\sqrt{2} & n = 0,1 \\ 0 & \text{otherwise} \end{cases} \quad h_{\psi}(n) = \begin{cases} 1/\sqrt{2} & n = 0 \\ -1/\sqrt{2} & n = 1 \\ 0 & \text{otherwise} \end{cases}$$

- $\{1, 4, -3, 0\} * \{-(1/2)^{0.5}, (1/2)^{0.5}\} = \{-(1/2)^{0.5}, -3(1/2)^{0.5}, 7(1/2)^{0.5}, -3(1/2)^{0.5}, 0\}$
- $W_{\psi}(1, k) = \{-3(1/2)^{0.5}, -3(1/2)^{0.5}\}$
- Or $W_{\psi}(1, k) = h_{\psi}(-n)W_{\varphi}(2, n) |_{n=2k, k \geq 0}$
 $= h_{\psi}(n)f(n) |_{n=2k, k \geq 0} = \sum_l h_{\psi}(2k-l)x(l) |_{k=0,1}$
 $= (1/2)^{0.5}x(2k) - (1/2)^{0.5}x(2k+1)$



7.4 Fast Wavelet Transform

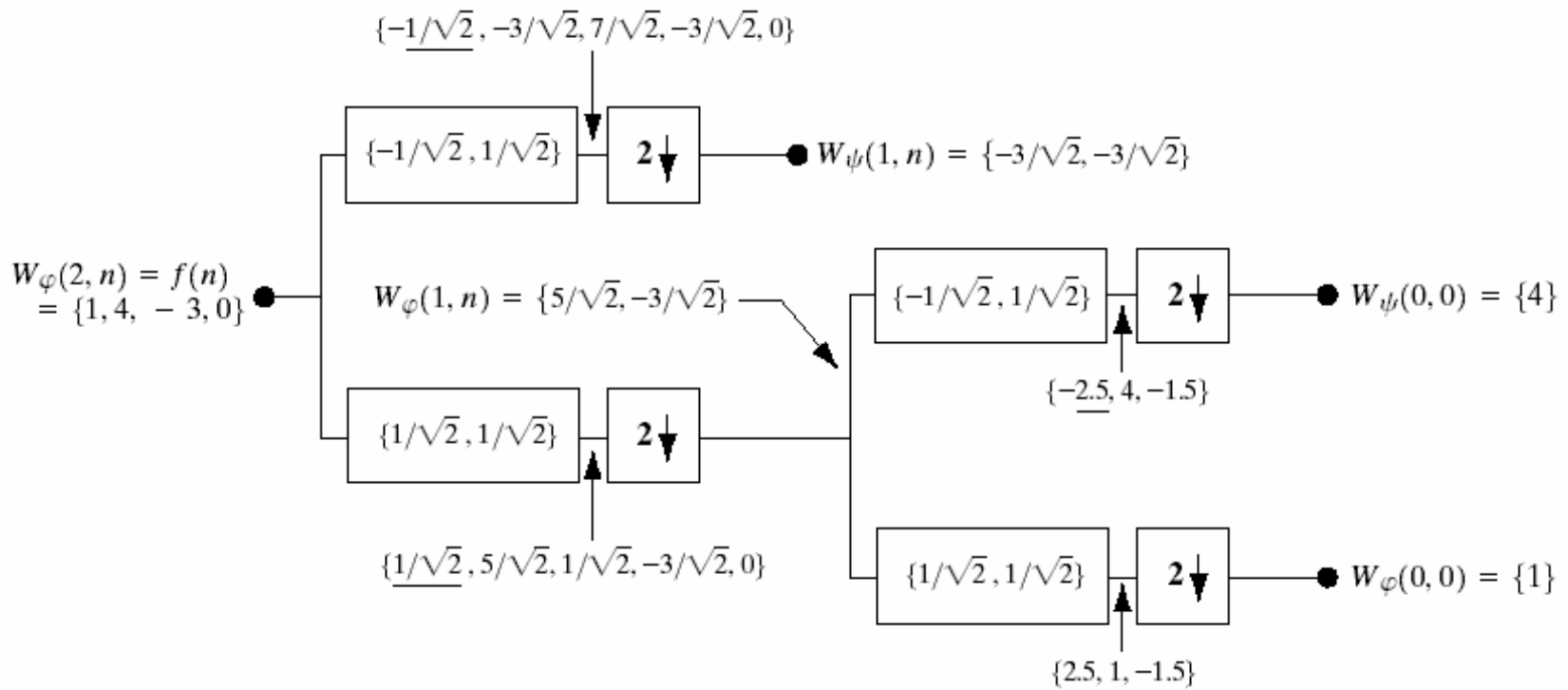
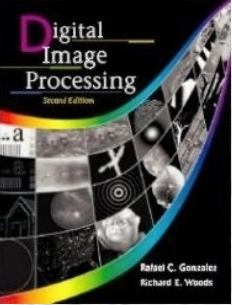


FIGURE 7.17 Computing a two-scale fast wavelet transform of sequence $\{1, 4, -3, 0\}$ using Haar scaling and wavelet vectors.



7.4 Fast Wavelet Transform- Inverse FWT

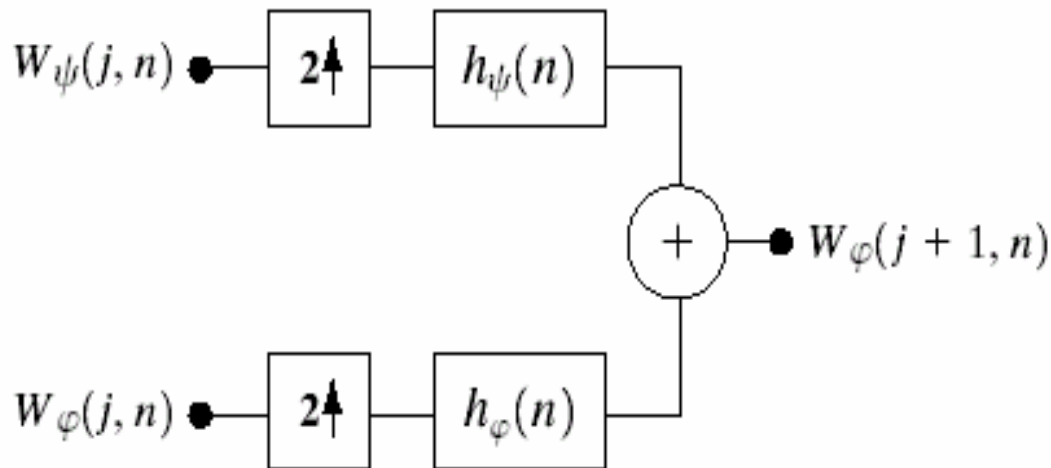
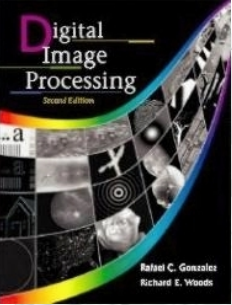


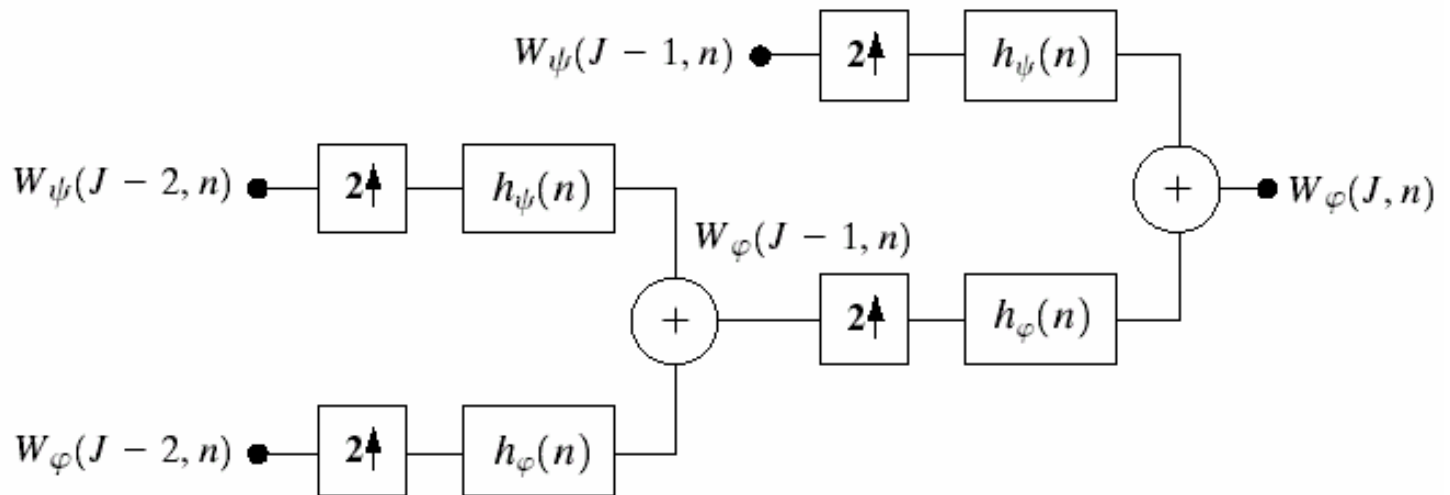
FIGURE 7.18 The FWT^{-1} synthesis filter bank.

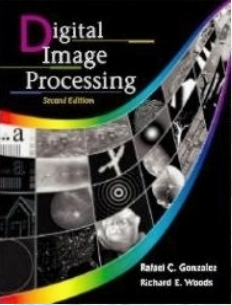
$$W_{\varphi}(j+1, k) = h_{\varphi}(k) \otimes W_{\varphi}^{up}(j, k) |_{k \geq 0} + h_{\psi}(k) \otimes W_{\psi}^{up}(j, k) |_{k \geq 0}$$



7.4 Fast Wavelet Transform- Inverse FWT

FIGURE 7.19 A two-stage or two-scale FWT^{-1} synthesis bank.





7.4 Fast Wavelet Transform- Inverse FWT

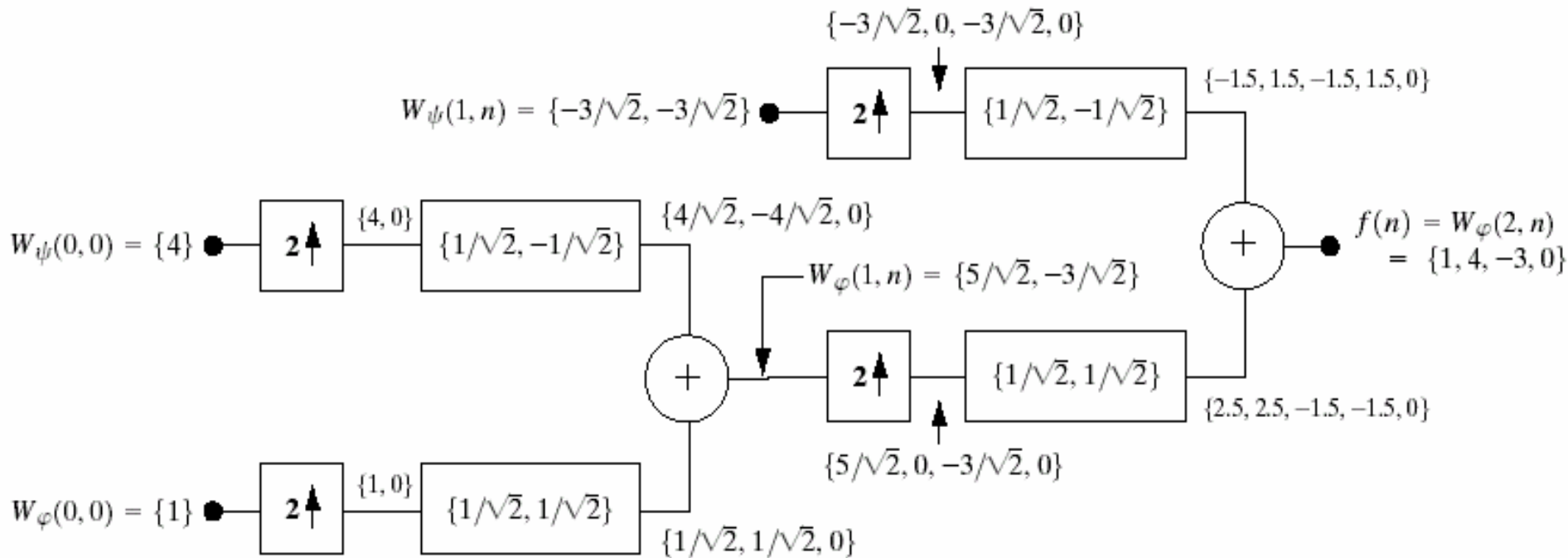
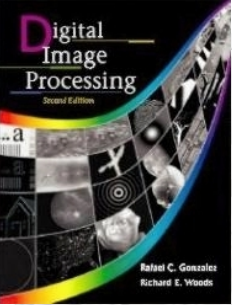
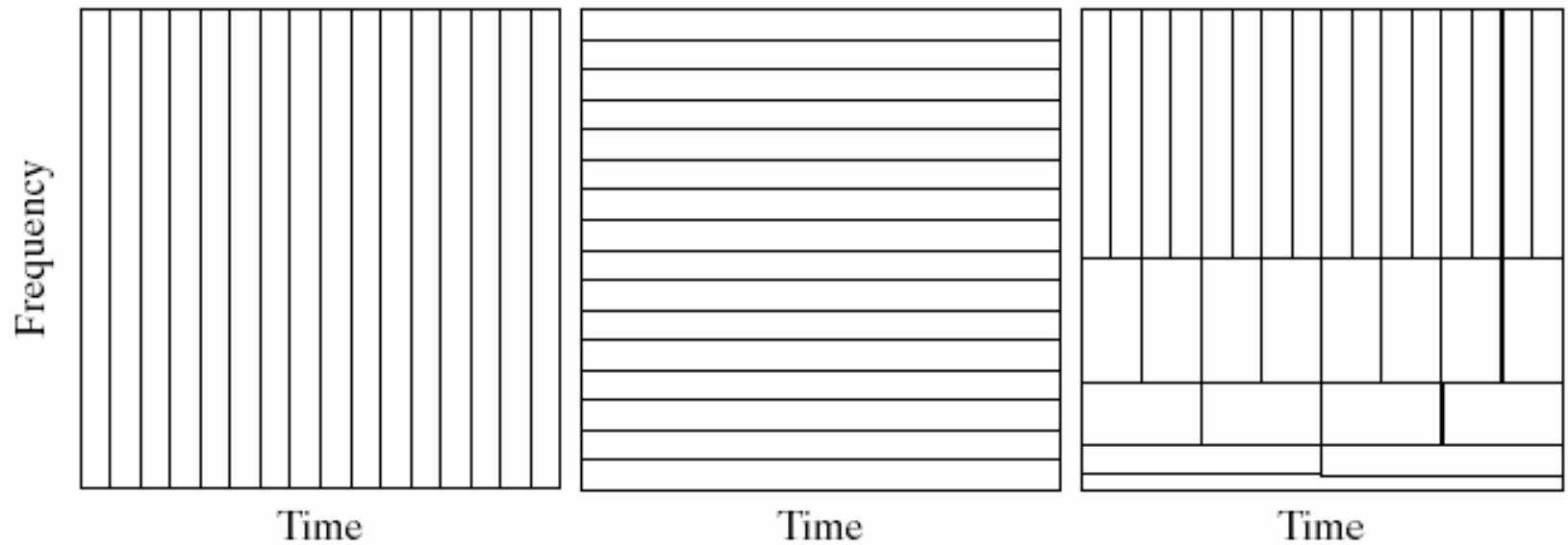


FIGURE 7.20 Computing a two-scale inverse fast wavelet transform of sequence $\{1, 4, -1.5\sqrt{2}, -1.5\sqrt{2}\}$ with Haar scaling and wavelet vectors.

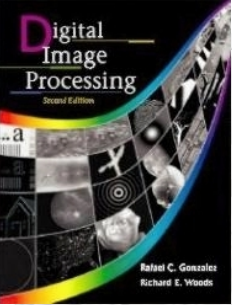


7.4 Fast Wavelet Transform- Inverse FWT



a b c

FIGURE 7.21 Time-frequency tilings for (a) sampled data, (b) FFT, and (c) FWT basis functions.



7.5 Wavelet transform in Two Dimension

- *2-D scaling function:*

$$\varphi(x, y) = \varphi(x) \varphi(y)$$

- *2-D wavelets:*

$$\psi^H(x, y) = \psi(x) \varphi(y)$$

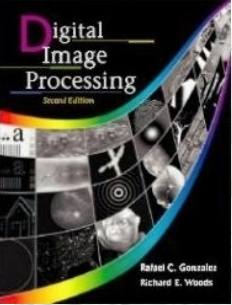
$$\psi^V(x, y) = \varphi(x) \psi(y)$$

$$\psi^D(x, y) = \psi(x) \psi(y)$$

- *Translated and scaled basis functions:*

$$\varphi_{j,m,n}(x, y) = 2^{j/2} \varphi(2^j x - m, 2^j y - n)$$

$$\psi_{j,m,n}^i(x, y) = 2^{j/2} \psi(2^j x - m, 2^j y - n), \quad i = \{H, V, D\}$$



7.5 Wavelet transform in Two Dimension

- The DWT of function $f(x,y)$ of size $M \times N$ is

$$W_{\varphi}(j_0, m, n) = \frac{1}{\sqrt{MN}} \sum_{x=0}^{M-1} \sum_{y=0}^{N-1} f(x, y) \varphi_{j_0, m, n}(x, y)$$

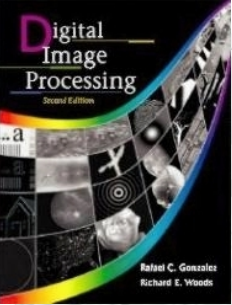
$$W_{\psi}(j_0, m, n) = \frac{1}{\sqrt{MN}} \sum_{x=0}^{M-1} \sum_{y=0}^{N-1} f(x, y) \psi_{j_0, m, n}^i(x, y)$$

where $i = \{H, V, D\}$

Normally we let $j_0 = 0$ and $M = N = 2^J$, $j = 0, 1, 2, \dots, J-1$

Inverse DWT

$$f(x, y) = \frac{1}{\sqrt{MN}} \sum_m \sum_n W_{\varphi}(j_0, m, n) \varphi_{j_0, m, n} + \frac{1}{\sqrt{MN}} \sum_{i=H, V, D} \sum_m \sum_n W_{\psi}(j_0, m, n) \psi_{j_0, m, n}^i$$



7.5 Wavelet transform in Two Dimension

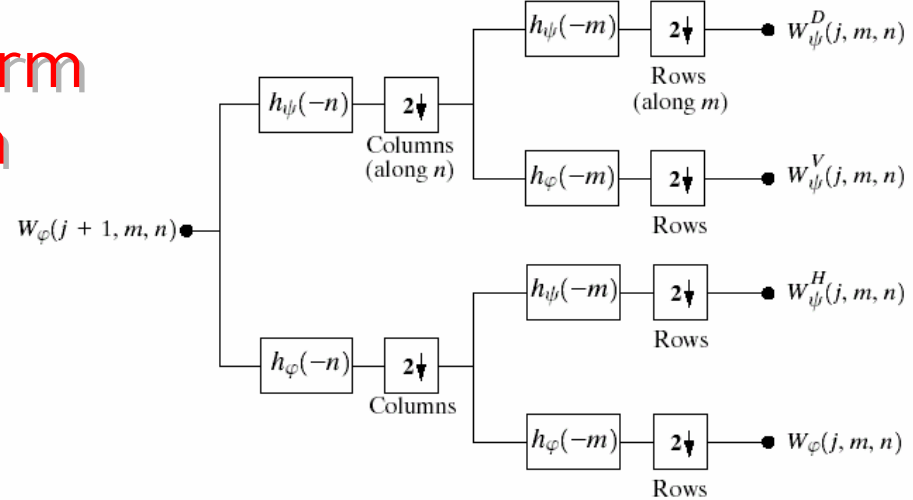
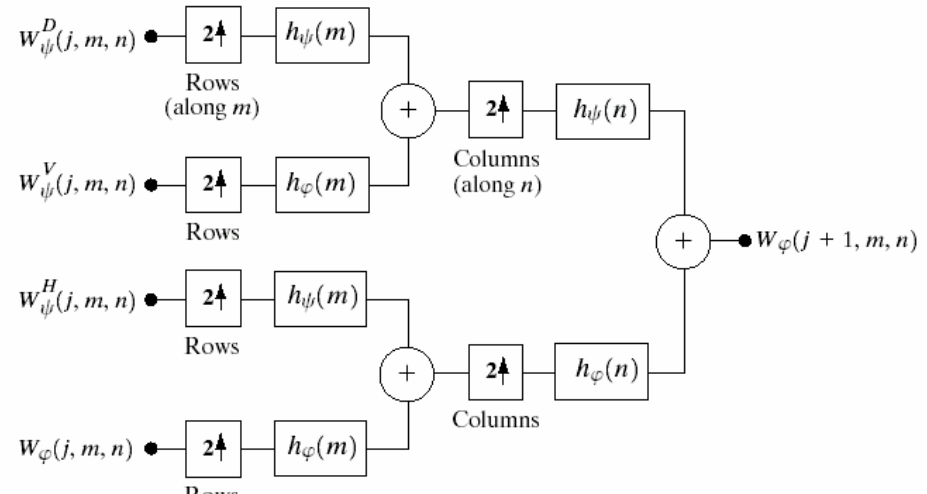
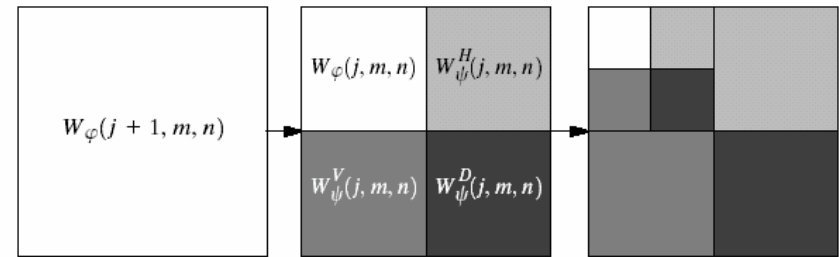
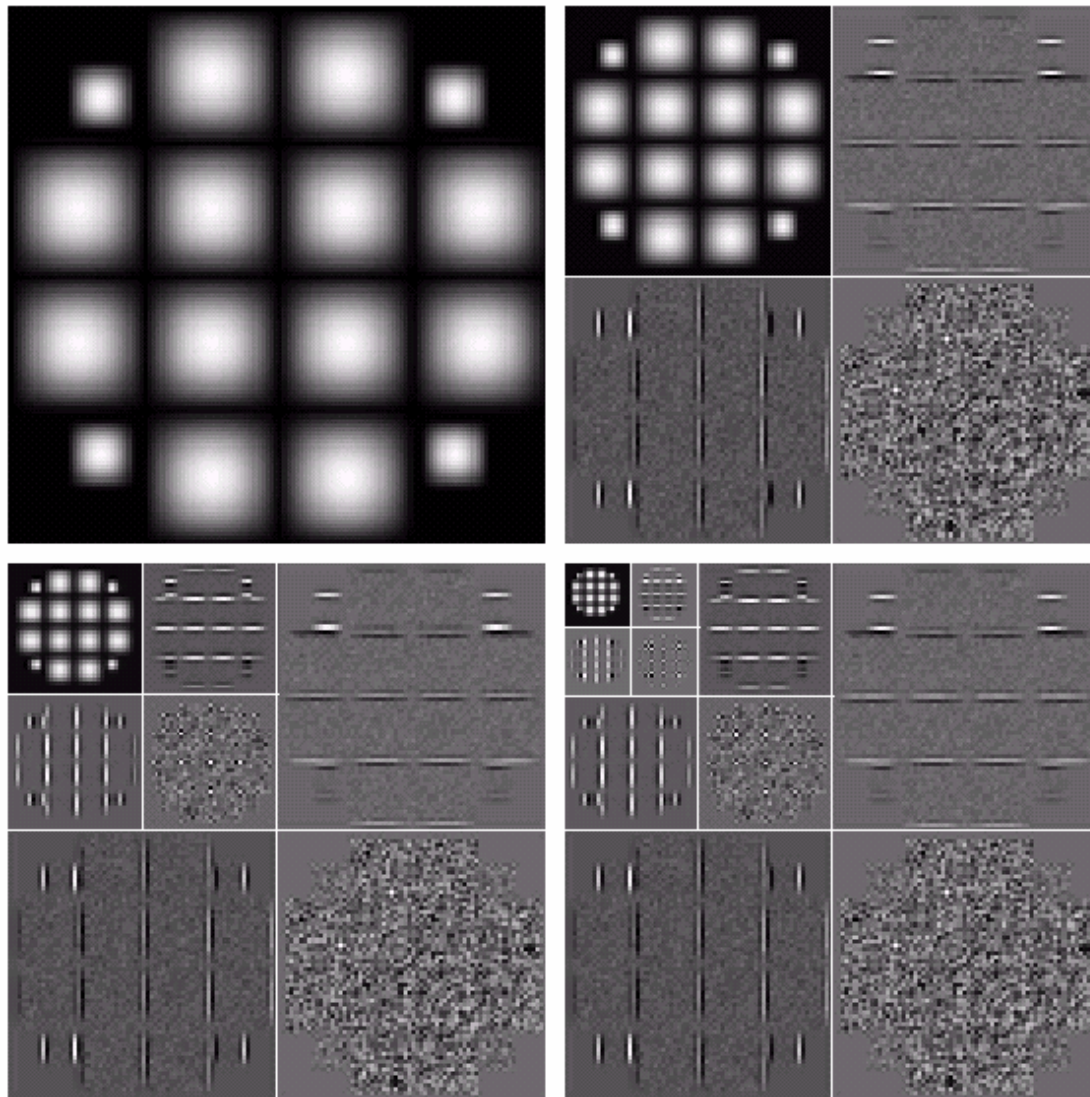


Figure 7.22 the 2-D fast wavelet transform (a) the analysis filter bank; (b) the results of decomposition; (c) the synthesis filter bank

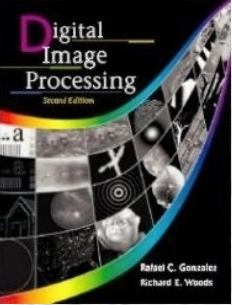


7.5 Wavelet transform in Two Dimension



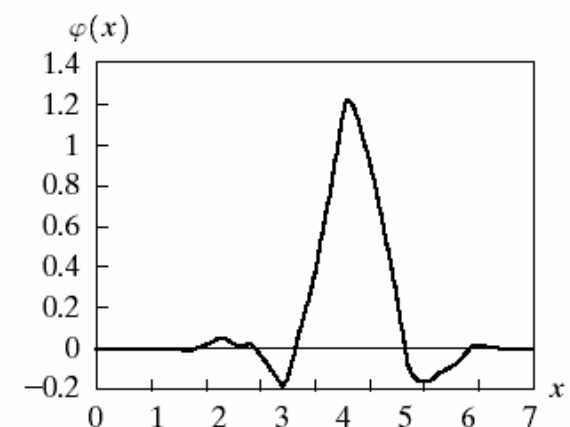
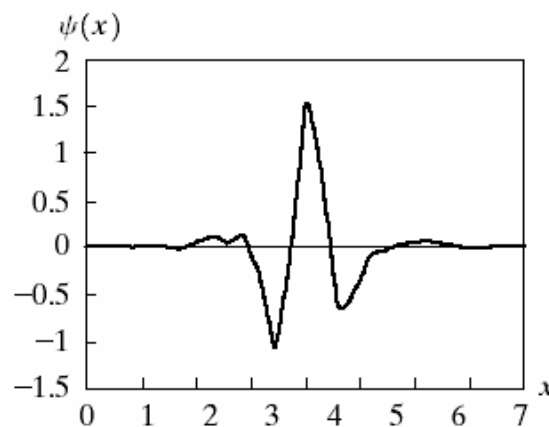
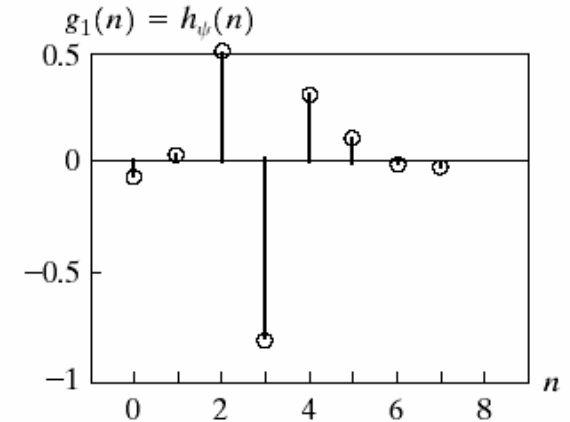
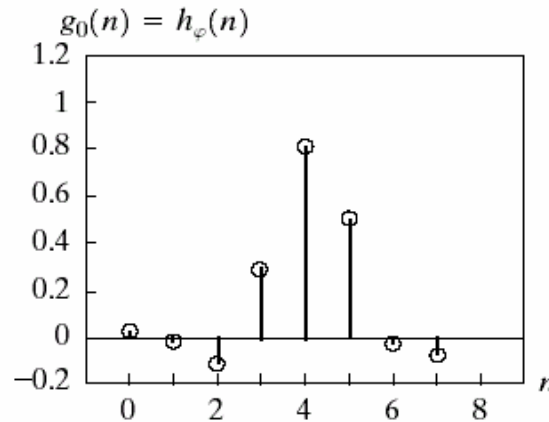
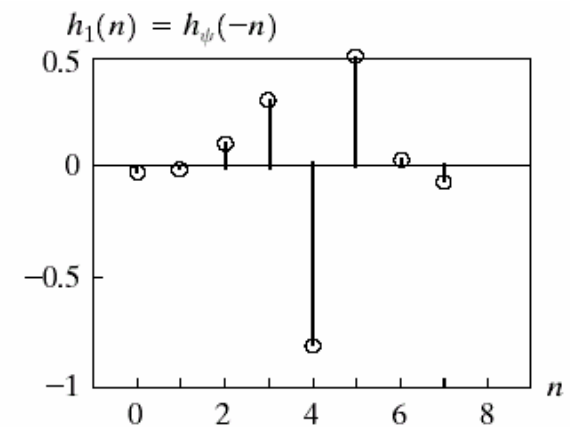
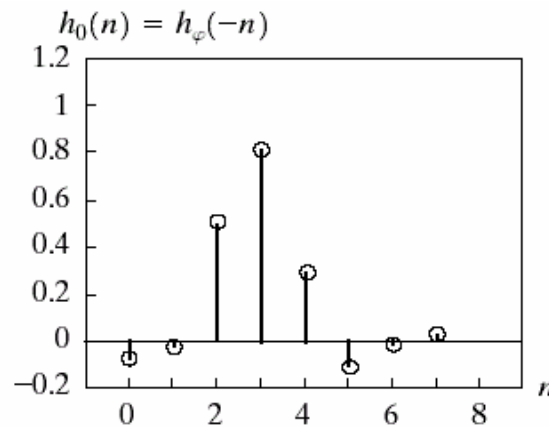
a	b
c	d

FIGURE 7.23 A three-scale FWT.

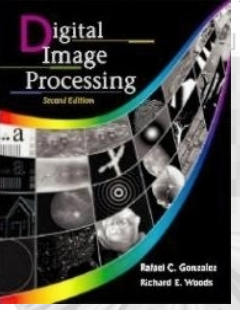


a b
c d
e f
g

FIGURE 7.24 Fourth-order symlets: (a)–(b) decomposition filters; (c)–(d) reconstruction filters; (e) the one-dimensional wavelet; (f) the one-dimensional scaling function; and (g) one of three two-dimensional wavelets, $\psi^H(x, y)$.

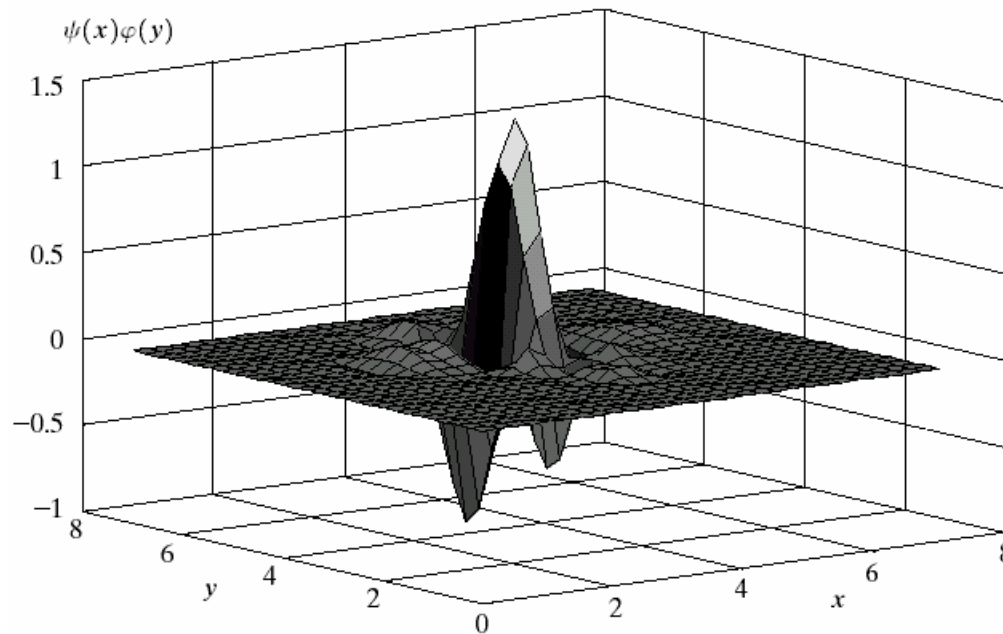


7.5 Wavelet transform in Two Dimension



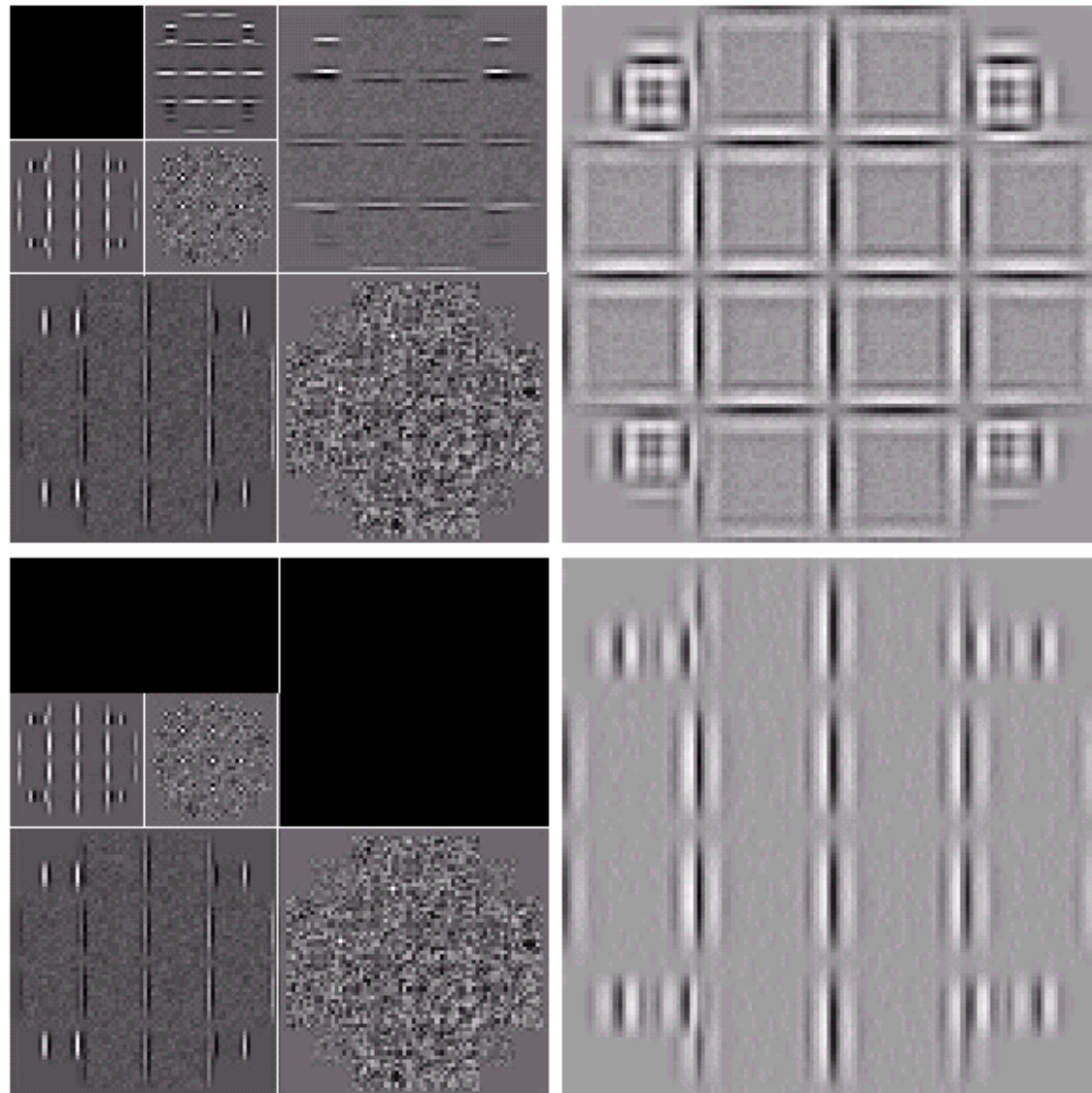
7.5 Wavelet Transform in Two Dimension

Fig. 7.24 (Con't)



7.5 Wavelet Transform in Two Dimension

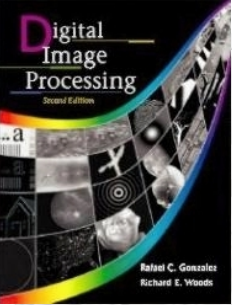
FIGURE 7.25
Modifying a DWT for edge detection: (a) and (c) two-scale decompositions with selected coefficients deleted; (b) and (d) the corresponding reconstructions.



DWT for edge detection

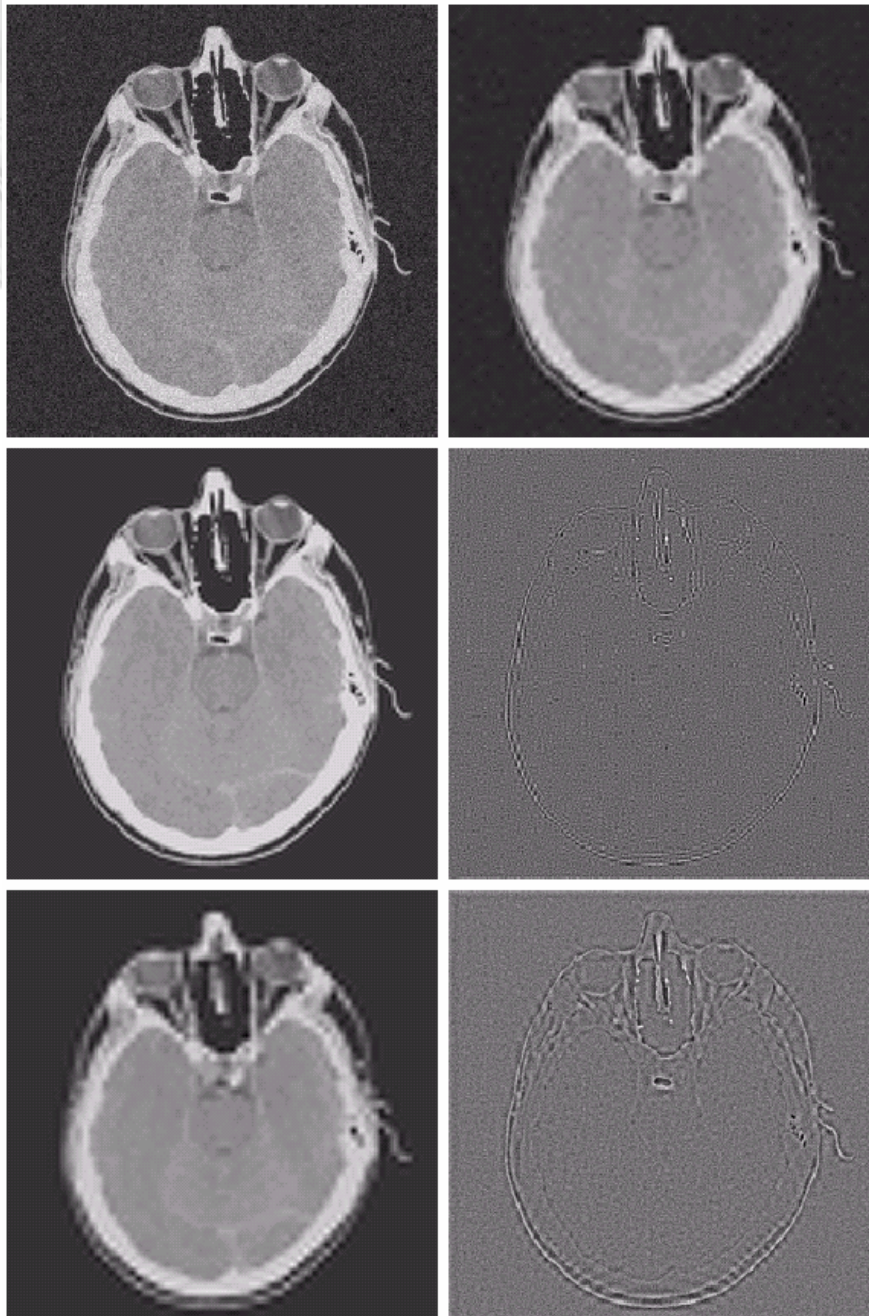
(a) Emphasize the reconstructed image edge

(b) Isolate the vertical edge



7.5 Wavelet Transform in Two Dimension

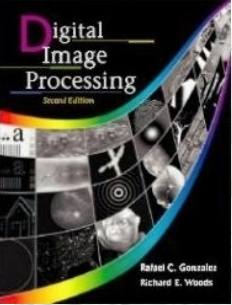
- The general wavelet-based for de-noising the image.
- Step 1: choose a wavelet and number of levels or scales, p , for decomposition, then compute FWT.
- Step 2: Thresholding the detail coefficients. Select and apply a threshold to the detail coefficients from scales $J-1$ to $J-P$. (a) Hard thresholding; (b) Soft thresholding, first hard-thresholding and then followed by scaling the nonzero coefficients toward zero to eliminate the discontinuity at the threshold.
- Step 3: Perform a wavelet reconstruction based on the original approximation coefficients at level $J-P$ and the modified detail coefficients for level from $J-1$ to $J-P$.



a b
c d
e f

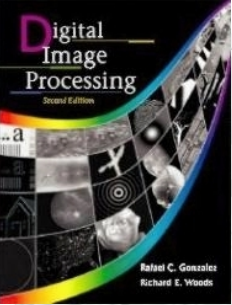
FIGURE 7.26
Modifying a DWT for noise removal: (a) a noisy MRI of a human head; (b), (c) and (e) various reconstructions after thresholding the detail coefficients; (d) and (f) the information removed during the reconstruction of (c) and (e). (Original image courtesy Vanderbilt University Medical Center.)

7.5 Wavelet Transform in Two Dimension

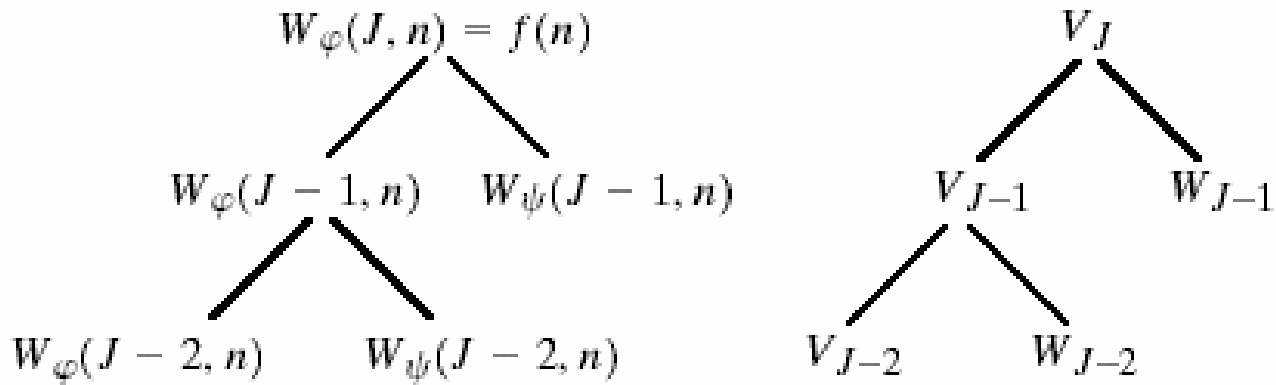


7.6 Wavelet packet

- DWT: the low frequencies are group into narrow bands, while the high frequencies are grouped into wider bands - constant-Q filters.
- **Wavelet packet** – a Generalized DWT, in which the details are teratively filtered and separated.
- Increased computation complexity raised from $O(M)$ to $O(M \log M)$



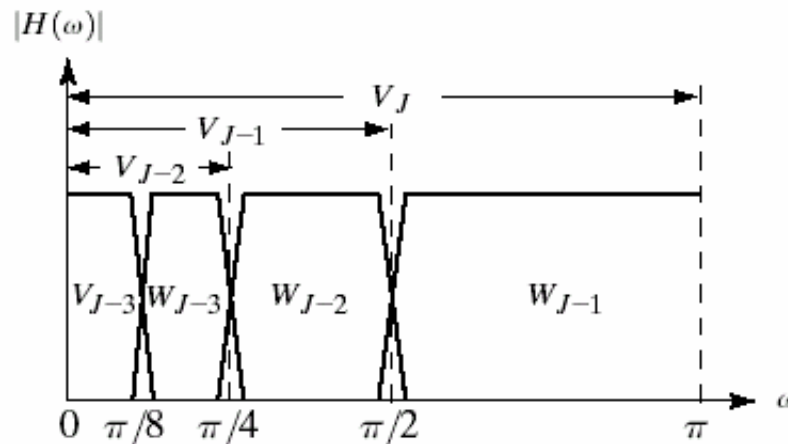
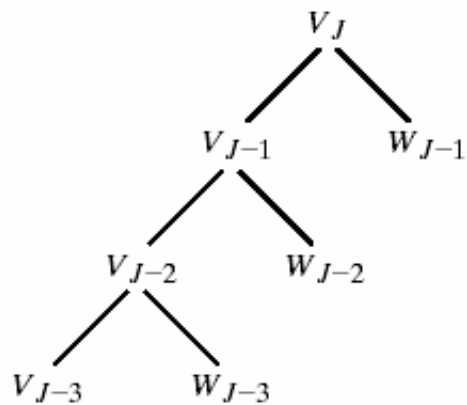
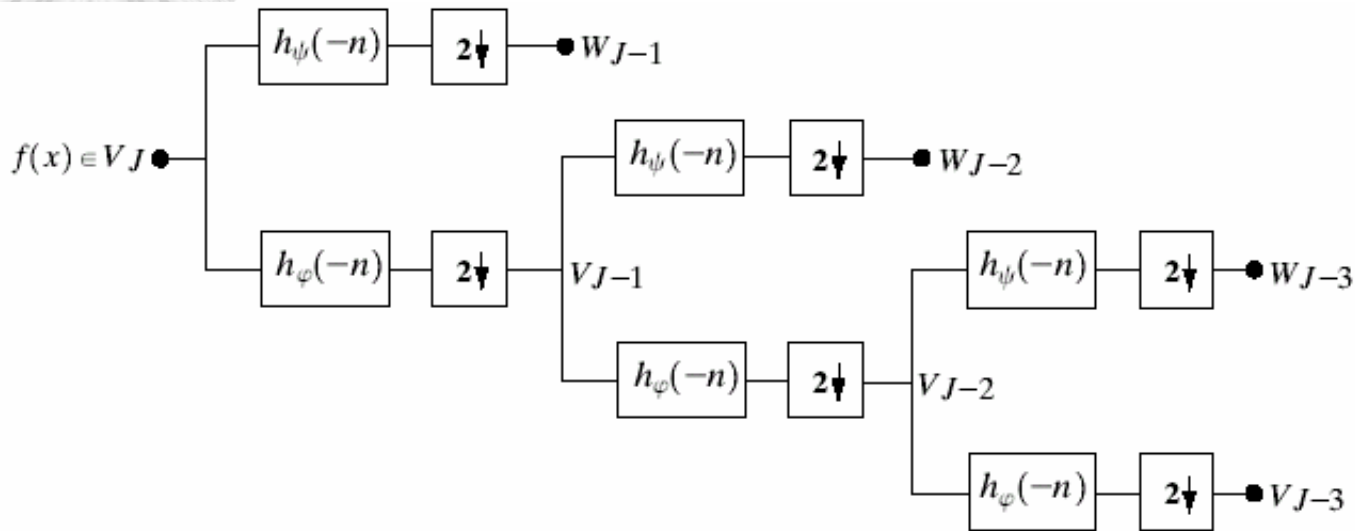
7.6 Wavelet packet



a b

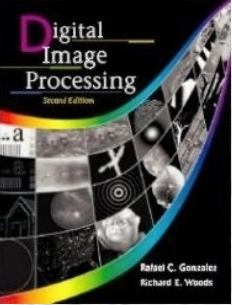
FIGURE 7.27 A coefficient (a) and analysis (b) tree for the two-scale FWT analysis bank of Fig. 7.16.

7.6 Wavelet packet



a
b c

FIGURE 7.28 A three-scale FWT filter bank: (a) block diagram; (b) decomposition space tree; and (c) spectrum splitting characteristics.



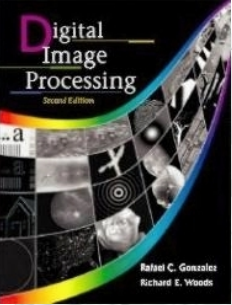
7.6 Wavelet packet

- Double subscripts are introduced for **Wavelet packet**
- The first identifies the scale of the FWT parent node, and the second is a variable length string of A's and D's.

A indicates the approximation filter.

D indicates the detail filter.

- This creates a fixed logarithmic relationship between the frequency bands.
- In general, P scale, 1-D wavelet packet transform support $D(P+1)=[D(P)]^2+1$ unique decompositions, where $D(1)=1$.



7.6 Wavelet packet

$$V_J = V_{J-3} \oplus W_{J-3} \oplus W_{J-2,A} \oplus W_{J-2,D} \oplus W_{J-1,AA} \oplus W_{J-1,AD} \oplus W_{J-1,DA} \oplus W_{J-1,DD}$$

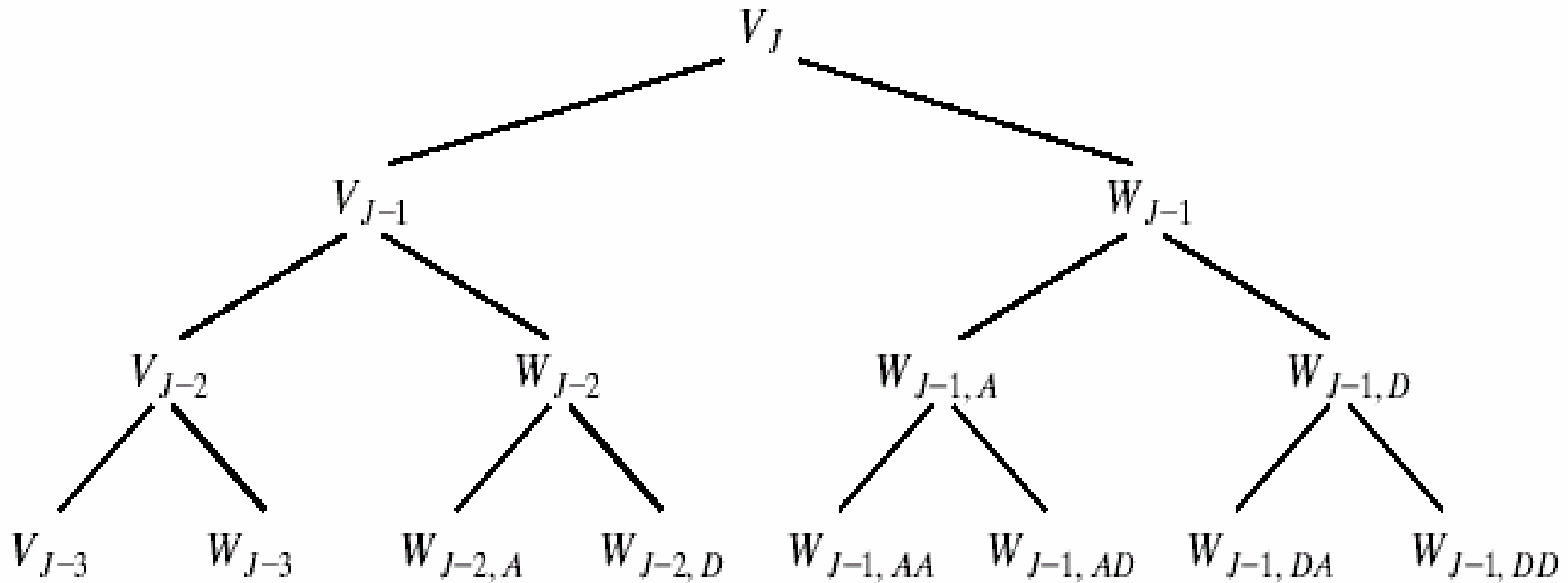
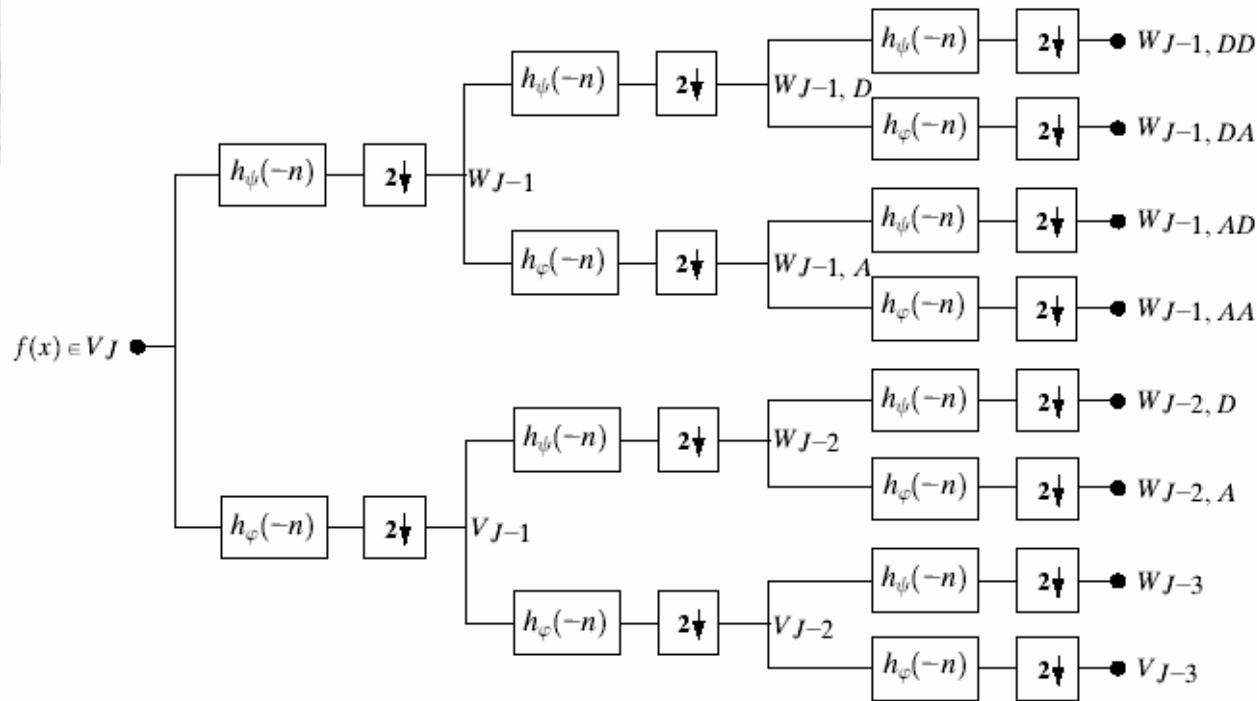


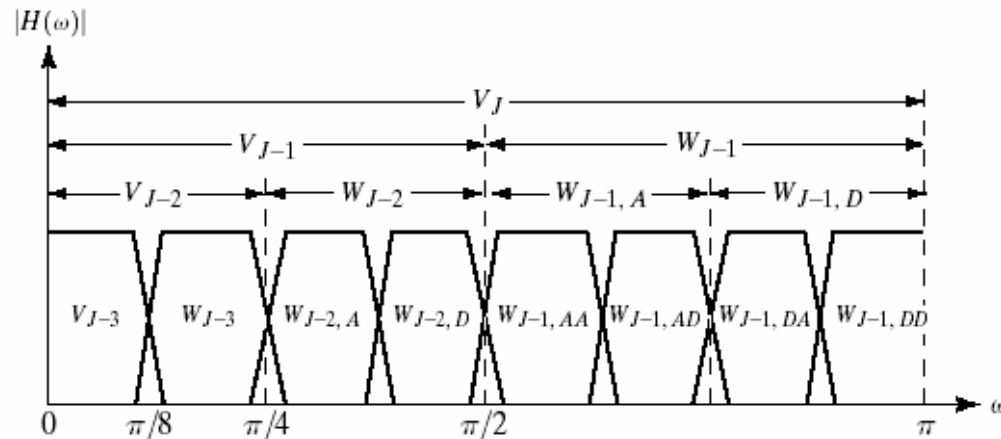
FIGURE 7.29 A three-scale wavelet packet analysis tree.

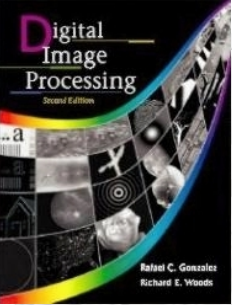
7.6 Wavelet packet



a
b

FIGURE 7.30 The (a) filter bank and (b) spectrum splitting characteristics of a three-scale full wavelet packet analysis tree.





7.6 Wavelet packet

$$V_J = V_{J-1} \oplus W_{J-1,D} \oplus W_{J-1,AA} \oplus W_{J-1,AD}$$

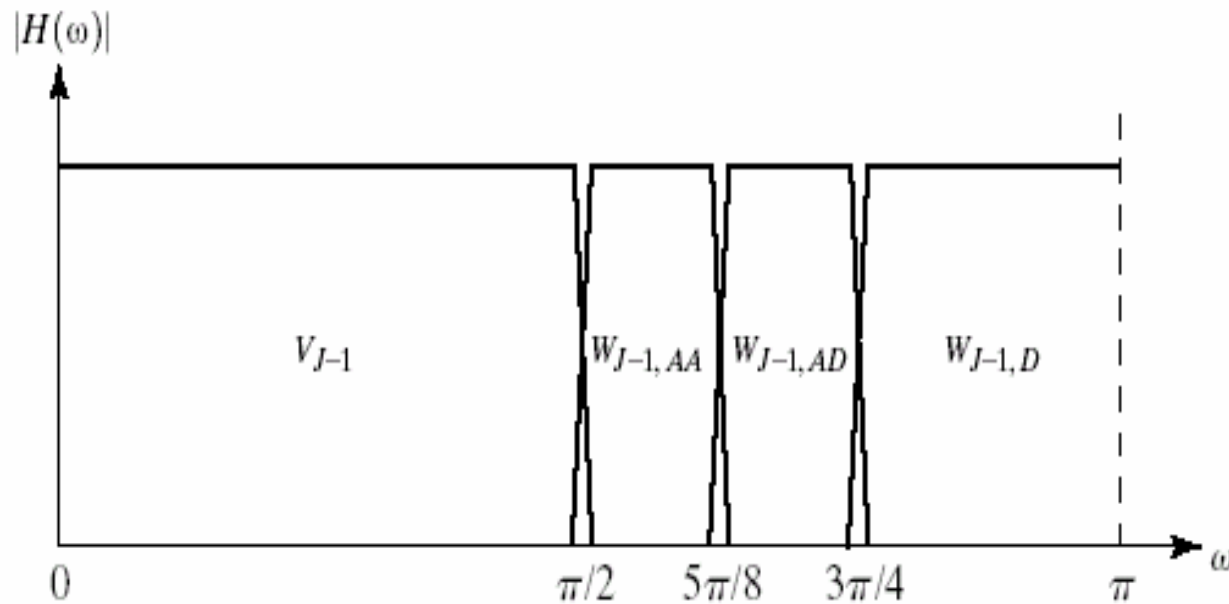
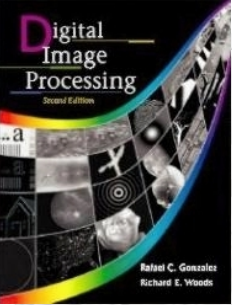
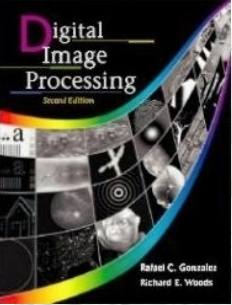


FIGURE 7.31 The spectrum of the decomposition in Eq. (7.6-5).



7.6 Wavelet packet

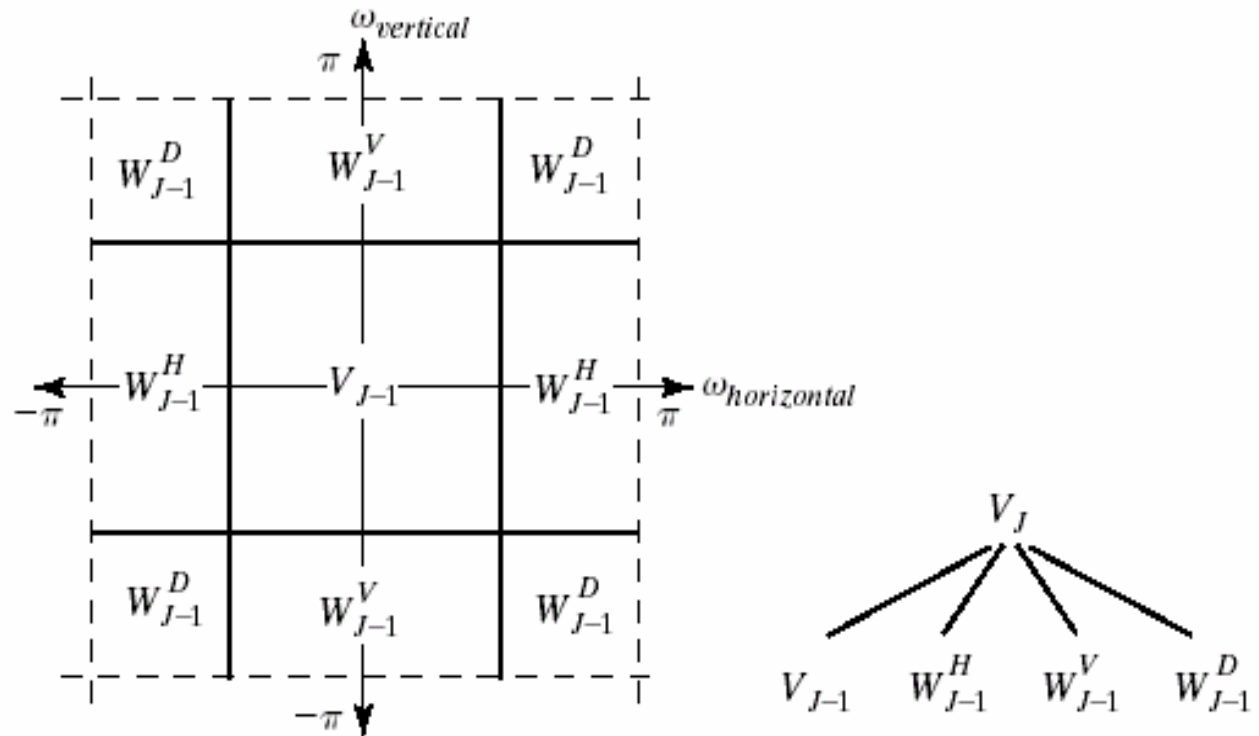
- The spectrum resulting from the first iteration ($j+1=J$) is shown in Figure 7.32
- It divides the frequency plane into four equal areas.
- Figure 7.33, a three-scale full wavelet packet decomposition.
- In general, A P -scale, 2-D wavelet packet transform support $D(P+1)=[D(P)]^4+1$ unique decompositions, where $D(1)=1$
- *Three-scale tree offer 83522 possible decompositions*

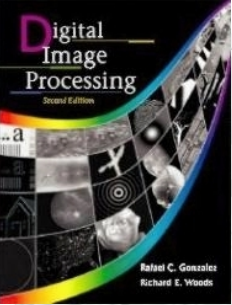


7.6 Wavelet packet

a b

FIGURE 7.32 The first decomposition of a two-dimensional FWT: (a) the spectrum and (b) the subspace analysis tree.





7.6 Wavelet packet

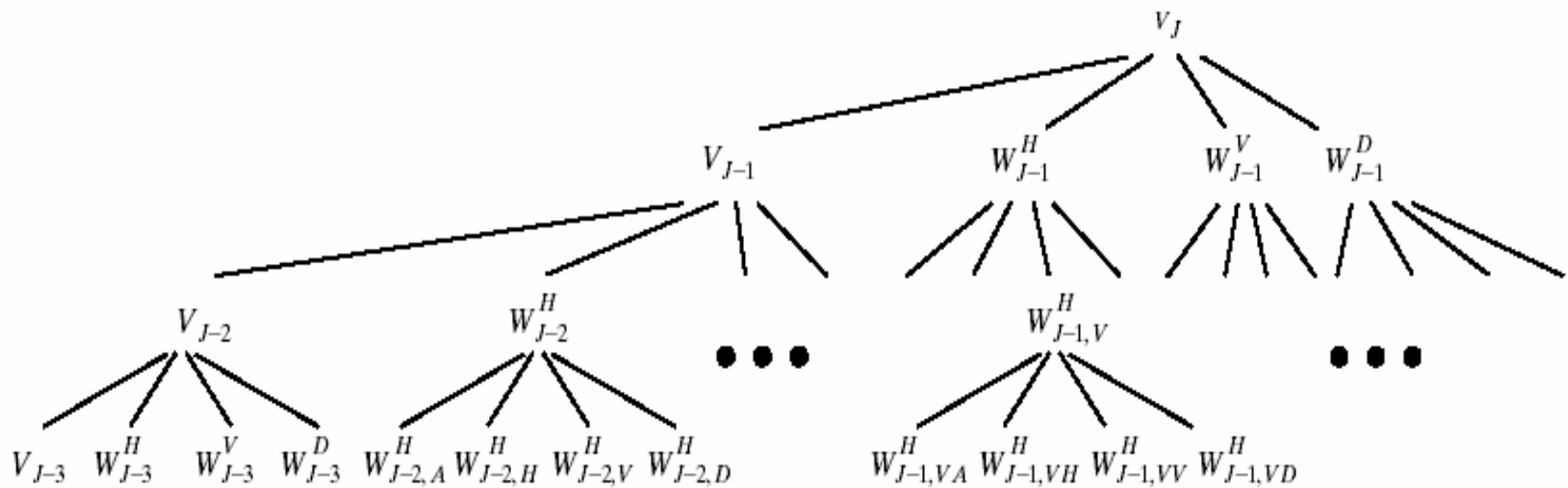
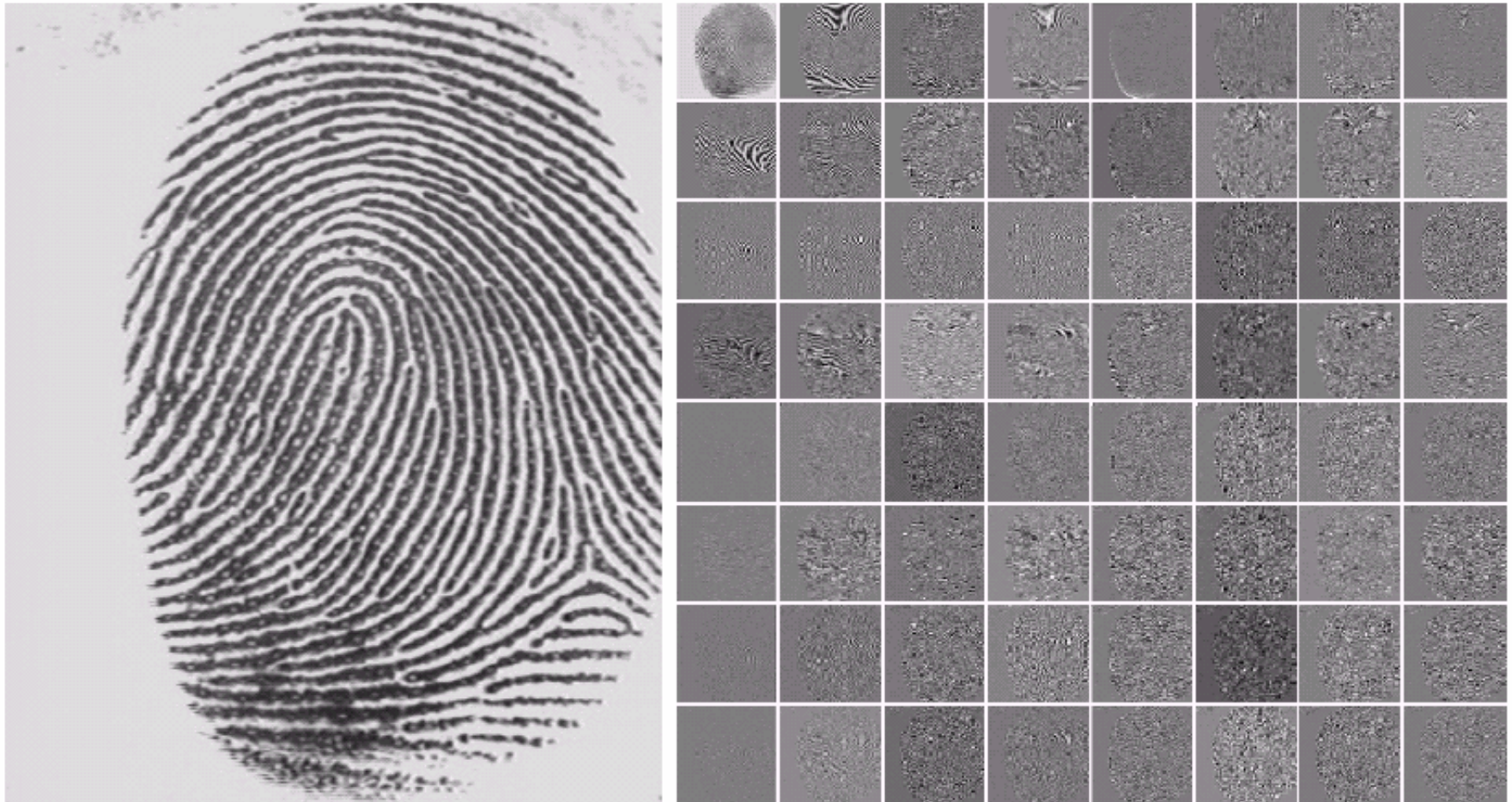


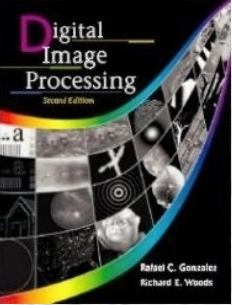
FIGURE 7.33 A three-scale, full wavelet packet decomposition tree. Only a portion of the tree is provided.

7.6 Wavelet packet



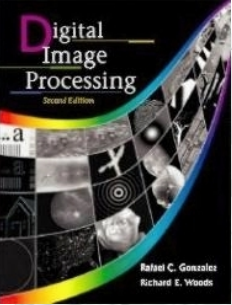
a b

FIGURE 7.34 (a) A scanned fingerprint and (b) its three-scale, full wavelet packet decomposition. (Original image courtesy of the National Institute of Standards and Technology.)



7.6 Wavelet packet

- To select a optimal decompositions for the compression of the image is considering the cost function $E(f)=\sum\Sigma/|f(x,y)|$, which measures the entropy or information content of 2-D function f .
- Minimal entropy leaf nodes should be favored because they have more near-zero values that lead to greater compression.
- The cost function $E(f)$ can be used as a local measurement for the node under consideration.



7.6 Wavelet packet

- For each node of the analysis tree
 - 1) compute both the entropy of the node E_P (parent entropy) and the entropy of the four offsprings, E_A , E_H , E_V , E_D .
 - 2) *Compare E_p with $E_A + E_H + E_V + E_D$, If the combined entropy is greater than the entrop of the parent than prune the offspring, keep only the parent.*

7.6 Wavelet packet

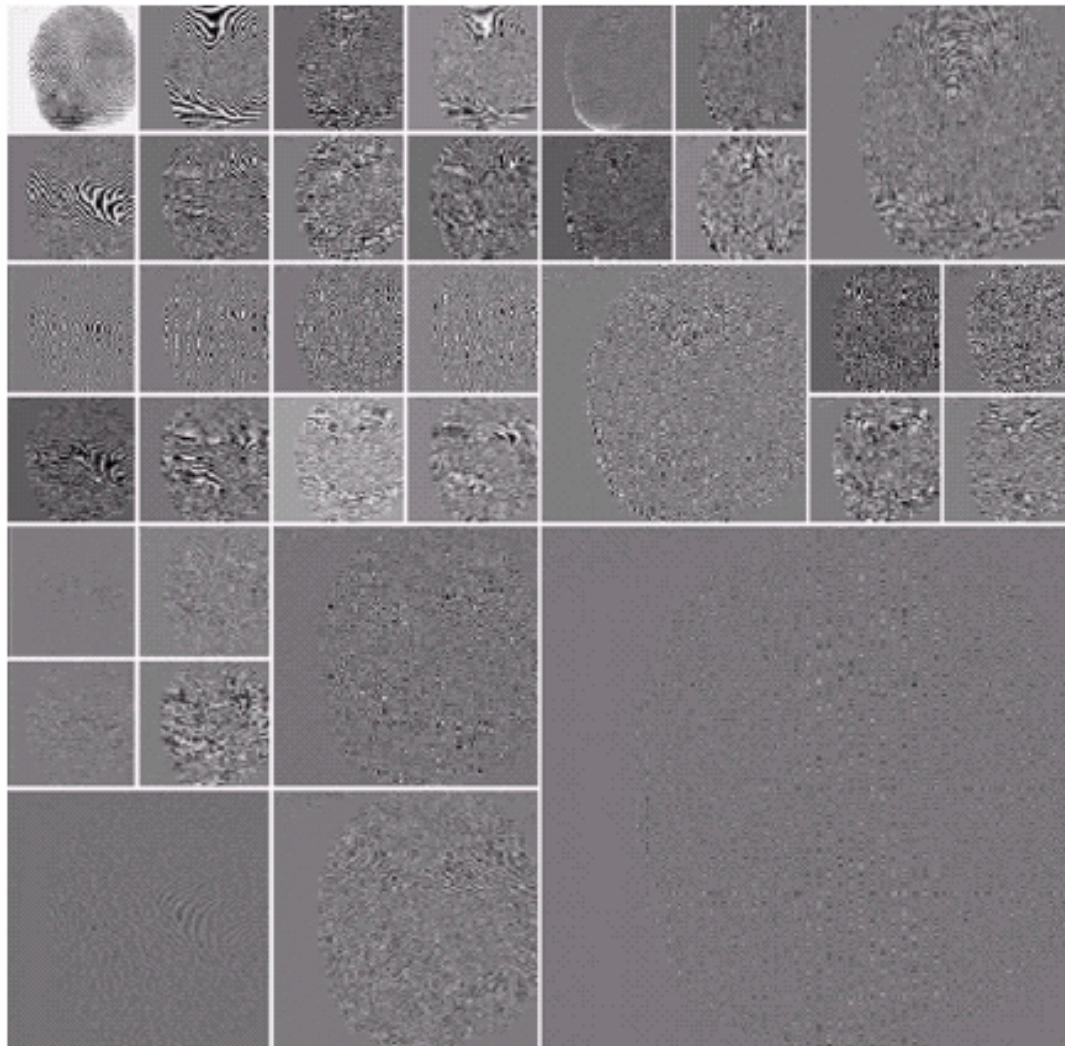


FIGURE 7.35 An optimal wavelet packet decomposition for the fingerprint of Fig. 7.34(a).

7.6 Wavelet packet

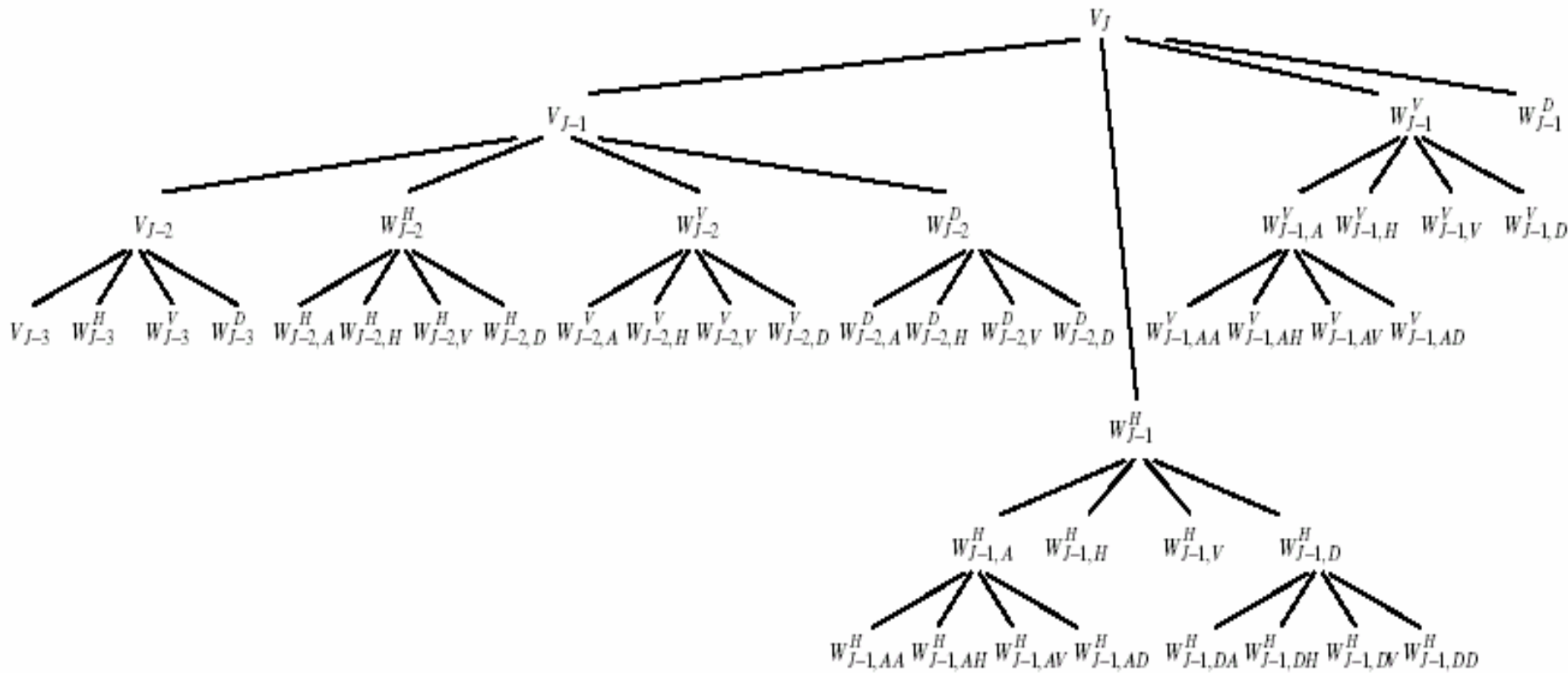
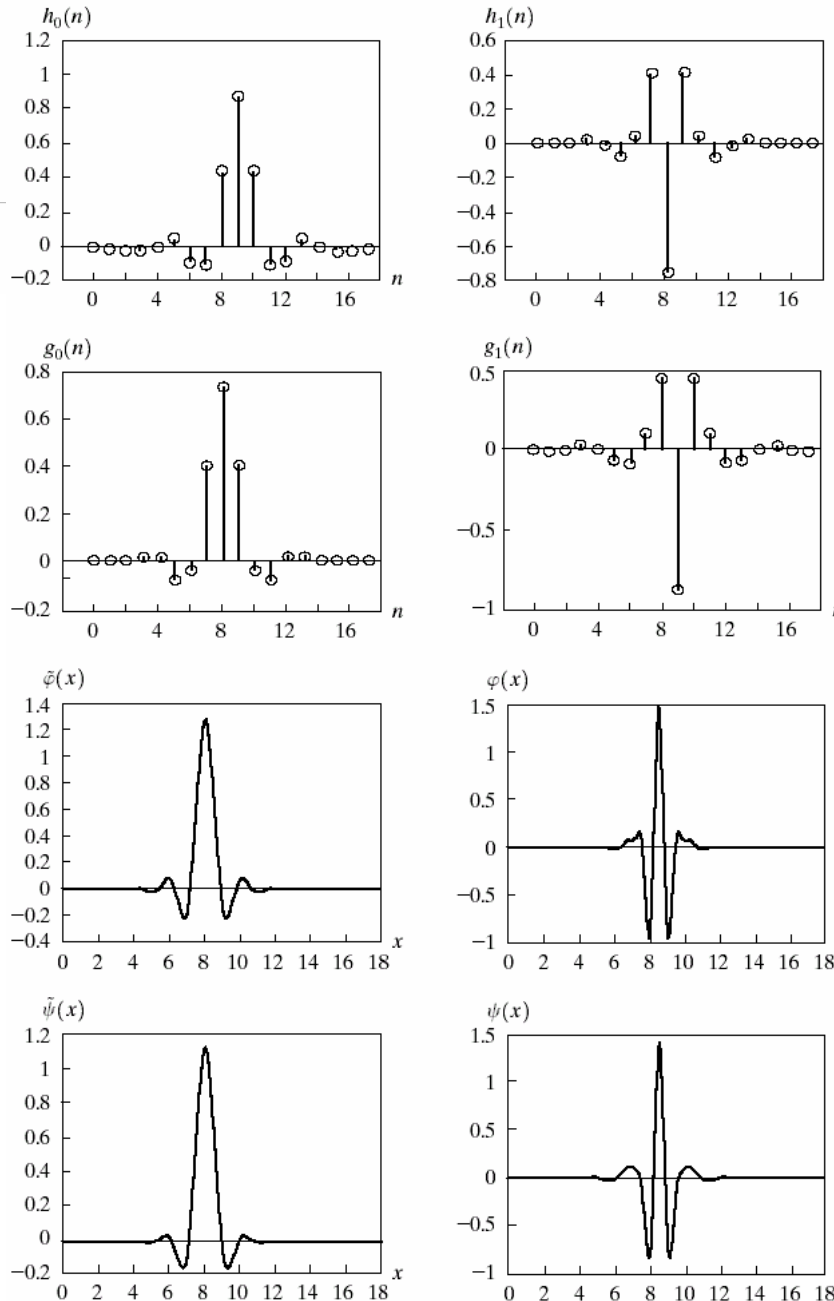
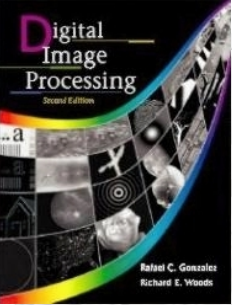


FIGURE 7.36 The optimal wavelet packet analysis tree for the decomposition in Fig. 7.35.



a b
c d
e f
g h

FIGURE 7.37 A member of the Cohen-Daubechies-Feauveau biorthogonal wavelet family: (a) and (b) decomposition filter coefficients; (c) and (d) reconstruction filter coefficients; (e)–(h) dual wavelet and scaling functions.

7.6 Wavelet packet